

RESEARCH ARTICLE

Voltage-Induced Ca^{2+} Release in Postganglionic Sympathetic Neurons in Adult Mice

Hong-Li Sun^{1,2}, Wen-Chin Tsai^{3,4}, Bai-Yan Li⁵, Wen Tao¹, Peng-Sheng Chen³, Michael Rubart^{1*}

1 Riley Heart Research Center, Herman B. Wells Center for Pediatric Research, Indiana University School of Medicine, Indianapolis, Indiana, United States of America, **2** Department of Pharmacology, Harbin Medical University-Daqing, Daqing, Heilongjiang, China, **3** The Krannert Institute of Cardiology and Division of Cardiology, Department of Medicine, Indiana University School of Medicine, Indianapolis, Indiana, United States of America, **4** Division of Cardiology, Department of Medicine, Hualein Tzu-Chi General Hospital, Hualein, Taiwan, **5** Department of Biomedical Engineering, Indiana University–Purdue University at Indianapolis, Indianapolis, Indiana, United States of America

* mrubartv@iu.edu



OPEN ACCESS

Citation: Sun H-L, Tsai W-C, Li B-Y, Tao W, Chen P-S, Rubart M (2016) Voltage-Induced Ca^{2+} Release in Postganglionic Sympathetic Neurons in Adult Mice. PLoS ONE 11(2): e0148962. doi:10.1371/journal.pone.0148962

Editor: Agustín Guerrero-Hernandez, Cinvestav-IPN, MEXICO

Received: December 24, 2014

Accepted: January 26, 2016

Published: February 9, 2016

Copyright: © 2016 Sun et al. This is an open access article distributed under the terms of the [Creative Commons Attribution License](https://creativecommons.org/licenses/by/4.0/), which permits unrestricted use, distribution, and reproduction in any medium, provided the original author and source are credited.

Data Availability Statement: All relevant data are within the paper and its Supporting Information files.

Funding: This work was supported by grants from the National Natural Science Foundation of China (81202509, <http://www.nsf.gov.cn/>) to HS and the National Heart, Lung and Blood Institute (R01HL07165, <http://www.nih.gov/>) to MR. The funders had no role in study design, data collection and analysis, decision to publish, or preparation of the manuscript.

Competing Interests: The authors have declared that no competing interests exist.

Abstract

Recent studies have provided evidence that depolarization in the absence of extracellular Ca^{2+} can trigger Ca^{2+} release from internal stores in a variety of neuron subtypes. Here we examine whether postganglionic sympathetic neurons are able to mobilize Ca^{2+} from intracellular stores in response to depolarization, independent of Ca^{2+} influx. We measured changes in cytosolic $\Delta\text{F}/\text{F}_0$ in individual fluo-4 –loaded sympathetic ganglion neurons in response to maintained K^+ depolarization in the presence (2 mM) and absence of extracellular Ca^{2+} ($[\text{Ca}^{2+}]_e$). Progressive elevations in extracellular $[\text{K}^+]_e$ caused increasing membrane depolarizations that were of similar magnitude in 0 and 2 mM $[\text{Ca}^{2+}]_e$. Peak amplitude of $\Delta\text{F}/\text{F}_0$ transients in 2 mM $[\text{Ca}^{2+}]_e$ increased in a linear fashion as the membrane become more depolarized. Peak elevations of $\Delta\text{F}/\text{F}_0$ in 0 mM $[\text{Ca}^{2+}]_e$ were ~5–10% of those evoked at the same membrane potential in 2 mM $[\text{Ca}^{2+}]_e$ and exhibited an inverse U-shaped dependence on voltage. Both the rise and decay of $\Delta\text{F}/\text{F}_0$ transients in 0 mM $[\text{Ca}^{2+}]_e$ were slower than those of $\Delta\text{F}/\text{F}_0$ transients evoked in 2 mM $[\text{Ca}^{2+}]_e$. Rises in $\Delta\text{F}/\text{F}_0$ evoked by high $[\text{K}^+]_e$ in the absence of extracellular Ca^{2+} were blocked by thapsigargin, an inhibitor of endoplasmic reticulum Ca^{2+} ATPase, or the inositol 1,4,5-triphosphate (IP_3) receptor antagonists 2-aminoethoxydiphenyl borate and xestospongine C, but not by extracellular Cd^{2+} , the dihydropyridine antagonist nifedipine, or by ryanodine at concentrations that caused depletion of ryanodine-sensitive Ca^{2+} stores. These results support the notion that postganglionic sympathetic neurons possess the ability to release Ca^{2+} from IP_3 -sensitive internal stores in response to membrane depolarization, independent of Ca^{2+} influx.

Introduction

Calcium ions play an important role in regulating a variety of neuronal processes, including excitability, gene transcription, synaptic plasticity, growth cone behavior, synaptogenesis, and neurotransmitter release [1,2]. Neurons use both extracellular and intracellular sources of calcium. Whereas voltage-gated calcium channels and receptor-operated channels such as the NMDA receptors enable Ca²⁺ influx from the extracellular space, inositol 1,4,5-trisphosphate (IP₃) receptors and ryanodine receptors distributed throughout the endoplasmic reticulum membrane are responsible for releasing Ca²⁺ from its internal stores [1]. The mechanism for triggering Ca²⁺ discharge from internal stores is unknown in some cases, and it is often assumed that Ca²⁺-induced Ca²⁺ release secondary to Ca²⁺ entry is the prevailing mechanism underlying Ca²⁺ mobilization. More recent studies, however, provide evidence for the existence of a Ca²⁺ influx-independent, voltage-induced Ca²⁺ release mechanism in neurons. A skeletal muscle excitation-contraction coupling-like mechanism, wherein conformational changes of the dihydropyridine receptor directly gate the ryanodine receptor, has been reported for hippocampal neurons [3], hypothalamic magnocellular neurons [4], and ischemically injured spinal cord white matter [5]. On the other hand, voltage-induced, Ca²⁺ influx-independent, Ca²⁺ release from IP₃-sensitive stores has been reported for insect dorsal unpaired median neurons [6]. Overall, these studies suggest the possibility that voltage-induced Ca²⁺ release from internal stores may be a more general phenomenon in neurons than previously thought.

Sympathetic ganglion neurons have been demonstrated to express both dihydropyridine-sensitive L-type calcium channels [7–10] and ryanodine receptors [11,12], suggesting the possibility that a skeletal muscle-like, voltage-induced Ca²⁺ release occurs in these cells. Here, we tested the hypothesis that sympathetic ganglion neurons in adult mice possess the ability to mobilize Ca²⁺ from internal stores in response to membrane depolarization, independent of Ca²⁺ influx. Our results provide, to the best of our knowledge, the first evidence that postganglionic sympathetic neurons are capable of releasing Ca²⁺ from internal stores in response to prolonged depolarization in the absence of extracellular calcium. Surprisingly, however, this process does not require dihydropyridine or ryanodine receptors. Rather, depolarization causes Ca²⁺ release from IP₃-sensitive internal stores, utilizing a yet to be identified plasmalemmal voltage sensor. This process may constitute a novel mechanism coupling electrical activity to a rise in intracellular Ca²⁺ in sympathetic neurons.

Materials and Methods

Preparation of sympathetic neurons

Sympathetic neurons were prepared in a manner previously described [13]. DBA/J mice at 2 to 3 months of age were sacrificed by cervical dislocation. The superior and stellate ganglia were removed under stereomicroscopy and immediately placed in chilled (4–8°C) sympathetic complete medium [DME-F12 medium supplemented with sodium bicarbonate, HEPES, penicillin/streptomycin, 5% fetal bovine serum, and MITO⁺ Serum extender (Collaborative Res, Bedford, MA, USA)]. The ganglia were then incubated for 20 min at 37°C in a Earle's Balanced Salt solution (Sigma, St. Louis, MO, USA) containing 10 U/ml papain (Worthington Biochemical Corp., Lakewood, NJ, USA), followed by a 30-min incubation in Earle's Balanced Salt solution supplemented with 1.3 mg/ml type II collagenase (Worthington) and 2.2 mg/ml dispase II (Roche, Indianapolis, IN, USA). Cells were then dissociated by trituration with a fire-polished glass Pasteur pipette in trituration solution (sympathetic complete medium containing 1.8 mg/ml bovine serum albumin) and plated on poly-D-lysine-coated No.1 circular glass cover slips. The isolated neurons were maintained in 5% CO₂-95% O₂ at 37°C in trituration solution and

used ~24 hours after plating. All procedures were approved by the Indiana University School of Medicine Institutional Animal Care and Use Committee.

Cytosolic Ca^{2+} imaging

A coverslip containing sympathetic neurons was transferred to a 263- μl recording chamber (model RC-21BRFS, Warner Instruments, Hamden, CT). Cells were loaded at room temperature with fluo-4 by incubation with the acetoxymethyl (AM) ester form of the dye (fluo-4/AM; Life Technologies, Grand Island, NY) at a final concentration of 2 μM in normal Tyrode's solution. After 20 min, cells were washed several times with dye-free Tyrode's solution and transferred to an inverted microscope (Axioscope) equipped with a Zeiss x63 1.4 numerical aperture water immersion lens. The microscope was attached to a confocal laser-scanning unit (Zeiss LSM 510). Fluo-4 fluorescence was probed every second by illumination with 488-nm laser light and emission was detected between 500 and 550 nm. The diameter of the pinhole was set to its maximum for all measurements. Images were taken in frame-mode at a pixel density of 512 x 512. Fluorescence signals were digitized at 8-bit resolution and analyzed using MetaMorph software (Molecular Probes, Sunnyvale, CA). To quantitate amplitude and time course of changes in cytosolic fluo-4 fluorescence, i.e., Ca^{2+} , signal intensities of pixels located inside the neuron soma (excluding the nuclei) were measured, spatially averaged, and background corrected [$F(t)$]. Background fluorescence was measured as the average of a 40 x 40 pixel cell-free area outside the neuron soma of interest in each frame of every time series. Baseline fluorescence intensity (F_0) was determined by averaging F over the 10-s interval preceding the cell's exposure to elevated $[\text{K}^+]_e$ in the extracellular medium ($[\text{K}^+]_e$), and the time course of normalized fractional dye fluorescence [$\Delta F/F_0(t)$] was obtained, where ΔF equals $F(t) - F_0$. Signal correction for bleaching was not necessary.

Cells were exposed to a high $[\text{K}^+]_e$ solution (40, 60, 80 or 100 mM KCl) in the presence of 2 mM Ca^{2+} for 30 s, followed by a 1-min exposure to normal Tyrode's solution. A second 30-s exposure to the same $[\text{K}^+]_e$ in the absence of extracellular Ca^{2+} (with 200 μM EGTA added to the extracellular solution) was applied, and then the high $[\text{K}^+]_e$ solution was replaced with Ca^{2+} -free normal Tyrode's solution. The first and second applications of high $[\text{K}^+]_e$ were separated by 3-min exposures to Ca^{2+} -free normal Tyrode's solution. Bath solution exchanges were performed via manual injections (~500 $\mu\text{l/s}$) through the input port of the perfusion chamber. For each consecutive bath fluid exchange in the experimental protocol, the injected volume was 7 ml, corresponding to ~27 times the chamber volume. Solution changes were rapid, based on the fast and steady change in membrane potential achieved when cells were exposed to external solutions with elevated $[\text{K}^+]_e$ (see Fig 1C). Nominally Ca^{2+} -free Tyrode's solution contained the following (in mM): 140 NaCl, 5 KCl, 1 MgCl_2 , 0.2 EGTA, 10 HEPES, and 10 D-glucose (pH 7.4). Assuming a 50 μM total contaminating Ca^{2+} , the free $[\text{Ca}^{2+}]_e$ was estimated to be ~43 nM [14,15]. For Ca^{2+} -containing Tyrode's solution, calcium was added (2 mM) and EGTA was omitted. When stimulating with elevated $[\text{K}^+]_e$, Na^+ was adjusted to maintain osmolarity [10,16]. Where indicated, drugs were added 20 min before and included throughout the stimulation. Pilot experiments demonstrated that the magnitude of the high $[\text{K}^+]_e$ -elicited Ca^{2+} response in Ca^{2+} -free bath solution gradually decreased with consecutive $[\text{K}^+]_e$ tests. Therefore, the response to one tandem only of high $[\text{K}^+]_e$ exposure (in 2 and 0 mM $[\text{Ca}^{2+}]_e$) was tested in an individual neuron.

Electrophysiology

Whole-cell voltage- and current-clamp recordings were performed at room temperature using a Multiclamp 700B patch-clamp amplifier (Molecular Devices, Sunnyvale, CA, USA). Patch

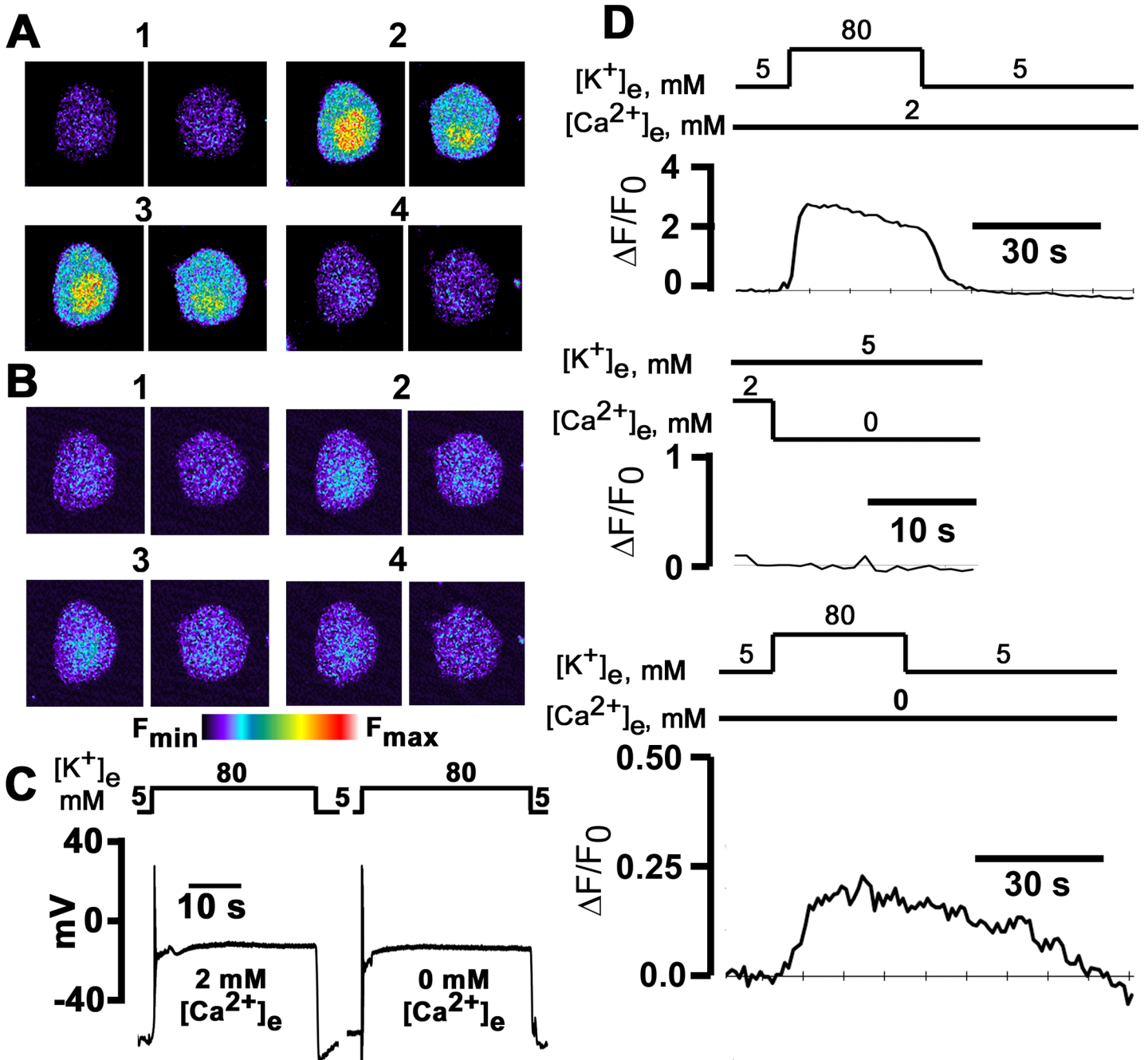


Fig 1. High [K⁺]_e-induced intracellular Ca²⁺ transients in the presence and absence of extracellular Ca²⁺. **A** and **B**: x-y fluorescence images recorded in 24 h cultured sympathetic ganglion neurons loaded with fluo-4/AM before, during and following 30-s depolarizations with 80 mM [K⁺]_e in 2 mM [Ca²⁺]_e (**A**) and in the absence of extracellular Ca²⁺ with 200 μM EGTA added to the extracellular solution (**B**). Exposure to elevated [K⁺]_e evoked transient increases in both cyto- and nucleoplasmic Ca²⁺ concentrations. Images in panels 2 and 3 were acquired at 10 and 30 s after initiating the [K⁺]_e challenge. **C**: High [K⁺]_e depolarizes the membrane potential both in the presence and absence of external Ca²⁺: 80 mM [K⁺]_e rapidly depolarized V_m from a resting membrane potential of -44 mV to 1 mV in 2 mM [Ca²⁺]_e, and from -41 mV to 0 mV in the absence of extracellular Ca²⁺. The level of depolarization was sustained for the duration of the [K⁺]_e challenge, both in the presence and absence of external Ca²⁺. **D**: Time courses of fractional fluorescence (ΔF/F₀), i.e., [Ca²⁺]_i, in the cytoplasm during exposure to 80 mM [K⁺]_e in the presence and absence of external Ca²⁺. ΔF/F₀ was calculated from the fluorescence intensity measured in the whole cytoplasm for each image taken every second.

doi:10.1371/journal.pone.0148962.g001

pipettes were pulled in a model P-97 puller (Sutter Instruments, Novato, CA, USA) from borosilicate glass capillaries and heat-polished prior to use with a Narishige MF-83 microforge (Narishige Inc., East Meadow, NY, USA). When filled with internal solution, the pipette resistance ranged from 2 to 5 MΩ. During the recording, changes in the bath solution were made by gravity driven perfusion. Pipette capacitance was zeroed on sealing. Whole-cell capacitive transients were compensated by 60–80%. Residual linear capacitive and leak currents were subtracted by the $-P/6$ method. Currents and voltages were low-pass filtered at 1 kHz and 5 kHz, respectively, using the built-in four-pole Bessel filter and sampled at 5 and 25 kHz, using a Digidata 1440A, acquired using Clampex10 and analyzed with Clampfit10 (all from Molecular Devices). Data collection was started ~2 to 3 min following membrane breakthrough.

Pipette solution for measuring whole-cell Ca²⁺ currents contained (in mM) 120 Cs-Aspartate, 1 MgCl₂, 4 MgATP, 0.3 Na₂GTP, 10 EGTA and 10 HEPES (pH 7.2), whereas the bath solution was composed of (in mM) 140 TEA-Cl, 2 MgCl₂, 2 CaCl₂, 10 glucose and 10 HEPES (pH 7.4). For measuring ion currents through voltage-gate Ca²⁺ channels in the absence of extracellular Ca²⁺, the bath solution contained (in mM) 140 NaCl, 2 MgCl₂, 0.2 EGTA, 10 glucose and 10 HEPES (pH 7.4). For measuring action potentials, the pipette solution contained (in mM) 145 K-Aspartate, 2 MgCl₂, 5 HEPES, 5 Na₂ATP and 1.1 EGTA (pH 7.2), and the bath solution consisted of (in mM) 140 NaCl, 5 KCl, 1 MgCl₂, 2 CaCl₂, 10 HEPES and 10 glucose (pH 7.4). For Ca²⁺-free bath solutions, calcium was omitted and EGTA (0.2 mM) was added. When recording the effects of elevating [K⁺]_e on membrane potential, [Na⁺] was lowered to maintain osmolarity. Osmolarities of all bath and pipette solutions were adjusted to 310 and 315 mOsm, respectively, using mannitol. Membrane potentials were adjusted for liquid junction potentials unless stated otherwise.

To characterize voltage dependence of peak I_{Ca} and to determine the I_{Ca} activation curve, currents were evoked by 300-ms pulses ranging from -90 to +60 mV in steps of 5 mV. The interval between voltage steps was 10 s. The peak $I_{Ca,L}$ density at each potential was plotted as a function of test voltage to generate the I - V curves. Activation curves were fitted with the following Boltzmann distribution equation: $G/G_{max} = 1/\{1 + \exp[(V_{1/2} - V)/k]\}$, where G is the voltage-dependent calcium conductance, G_{max} is the maximal calcium conductance, $V_{1/2}$ is the potential at which activation is half-maximal, V is the membrane potential, and k is the slope. G values were determined by the following equation: $G = I_{max}/(V - E_{Ca})$, where E_{Ca} is the reversal potential.

To examine steady-state inactivation, the voltage that gave maximal peak current was used for subsequent protocols. Cells were administered a series of prepulses (-90 to 40 mV) lasting 300 ms, from a holding potential of -90 mV, followed, after a 20-ms gap at -90 mV, by a 300-ms depolarization to a voltage eliciting the maximal peak current (0 mV). The interval between conditioning prepulses was 10 s. The resulting curves were normalized and fitted using the following Boltzmann distribution equation: $I/I_{max} = 1/\{1 + \exp[(V - V_{1/2})/k]\} + C$, where I_{max} is the peak current elicited after the most hyperpolarized prepulse, V is the preconditioning pulse potential, and C is a constant.

The membrane capacitance was calculated from 5-mV hyperpolarizing and depolarizing steps (20 ms) applied from a holding potential of -70 mV according to the equation: $C_M = \tau / \Delta V * I_0 / (1 - I_{\infty} / I_0)$, where C_M is membrane capacitance, τ is the time constant of the capacitance current relaxation, I_0 is the peak capacitive current determined by single exponential fit and extrapolation to the first sample point after the voltage step ΔV , and I_{∞} is the amplitude of the steady-state current during the voltage step [17]. Capacitive currents were sampled at 25 kHz and filtered at 5 kHz.

Data analysis

Summarized data are expressed as means \pm SEM. Statistical analyses were determined by paired *t*-test, unpaired *t*-test, and parametric and non-parametric one-way analyses of variance coupled with the appropriate *post hoc* analyses to determine significance ($P < 0.05$). Fisher Exact test was used to determine differences of proportions.

Chemicals

Stock solutions of 2-aminoethoxydiphenyl borate (2-APB), nifedipine, ryanodine and thapsigargin were prepared in DMSO. The final DMSO concentration in the experimental solution did not exceed 1 μ l/ml. Caffeine stock solution was prepared in ddH₂O. Stock solution of tetraakis (2-pyridylmethyl) ethylenediamine (TPEN) was prepared in ethanol, and xestospongine C stock solution was made in PBS.

Results

High [K⁺]_e-induced membrane depolarization evokes Ca²⁺ transients in mouse sympathetic ganglion neurons in the absence of extracellular Ca²⁺

Raising extracellular [K⁺] has been previously shown by others to produce stable and reproducible membrane depolarization in sympathetic ganglion neurons in culture, increasing intracellular free [Ca²⁺] in the presence of external Ca²⁺ [10]. Here, we combined [K⁺]_e depolarization with fluorescent Ca²⁺ imaging to examine the possibility that membrane depolarization evokes Ca²⁺ transients within isolated sympathetic ganglion neurons of adult mice not only in the presence of extracellular Ca²⁺ but also in its absence. Representative Ca²⁺ responses of two fluo-4/AM-loaded neurons elicited by consecutive 30-s exposures to 80 mM [K⁺]_e in the presence of 2 mM [Ca²⁺]_e and in Ca²⁺-free bath solution (with 200 μ M EGTA added) are illustrated in Fig 1A and 1B, respectively. Elevating [K⁺]_e in normal Ca²⁺ gave rise to increases in global fluorescence intensity, which were larger in the nuclei than in the cytosols (Fig 1A). The fluorescence signals remained elevated throughout the exposure to high [K⁺]_e (panels 2 and 3 in Fig 1A) and returned to baseline values following restoration of [K⁺]_e (panel 4 in Fig 1A). The [K⁺]_e challenge was repeated in the absence of extracellular Ca²⁺ following a 3-min exposure to Ca²⁺-free normal Tyrode's solution. As illustrated in Fig 1B, a second 30-s exposure to 80 mM [K⁺] in the absence of external Ca²⁺ gave rise to sustained elevations in intracellular Ca²⁺ (panels 2 and 3 in Fig 1B), although the magnitude of the effect was markedly reduced compared to the 2 mM [Ca²⁺]_e condition. Fluorescence signal intensity recovered upon restoration of [K⁺]_e in the continued absence of extracellular Ca²⁺.

To make certain that membrane depolarization evoked by 80 mM [K⁺]_e was maintained at similar potentials in the presence and absence of external Ca²⁺, the membrane potential was recorded from isolated sympathetic neurons before and during the 30-s depolarization. A representative example is shown in Fig 1C. Both in the presence and absence of extracellular Ca²⁺, high [K⁺]_e rapidly depolarized the neuron following the solution change, and remained stable while [K⁺]_e = 80 mM. The magnitude of depolarization appeared similar under both conditions. After [K⁺]_e was restored to 5 mM, membrane potential exhibited a transient afterhyperpolarization in 2 mM [Ca²⁺]_e. On average, the degree of membrane depolarization evoked by 80 mM [K⁺]_e in 0 mM [Ca²⁺]_e was slightly less than that in 2 mM [Ca²⁺]_e (see Table 1).

Next, we sought to quantitate the high [K⁺]_e-evoked changes in cytosolic Ca²⁺ level, using $\Delta F/F_0$ as a measure. Plots of $\Delta F/F_0$ as a function of time for one of the neurons in Fig 1A and 1B are displayed in Fig 1D. The neuron responds to high [K⁺]_e exposure with an initial peak

Table 1. Membrane potentials of sympathetic ganglion neurons at rest and during depolarization with elevated [K⁺]_e in normal [Ca²⁺]_e and in the absence of extracellular Ca²⁺ (with 200 μM EGTA added to the bath solution). Values are expressed as means ± SEM.

[K ⁺] _e , mM	2 mM [Ca ²⁺] _e , mV	0 mM [Ca ²⁺] _e , mV
5	-61.8 ± 4.4	-59.9 ± 3.1
40	-31.8 ± 1.4	-31.2 ± 0.7
60	-21.9 ± 0.9	-23.2 ± 0.9
80	-15.7 ± 0.5	-18.5 ± 0.8*
100	-11.5 ± 0.6	-14.2 ± 0.8*

*P<0.05 versus 2 mM [Ca²⁺]_e by paired t-test or Wilcoxon Signed Rank test.

doi:10.1371/journal.pone.0148962.t001

followed by a slow, spontaneous decay, which was seen in all cells tested, despite the fact that the depolarization of the plasma membrane was maintained throughout the 30-s [K⁺]_e challenge. Increases in ΔF/F₀ typically resolved within less than 15 s after restoration of [K⁺]_e. Replacement of normal Tyrode's solution with Ca²⁺-free solution did not evoke significant changes in cytosolic [Ca²⁺] (Fig 1D, middle panel), indicating that the solution change *per se* does not contribute to the rise in fluo-4 fluorescence seen in response to elevated [K⁺]_e in the absence of external Ca²⁺. A 30-s exposure of the same neuron to 80 mM [K⁺]_e in Ca²⁺-free bath solution evoked a low-amplitude Ca²⁺ transient which exhibited markedly slower rise and decay kinetics compared to the transient in 2 mM [Ca²⁺]_e (Fig 1D, lower panel). Overall, 47 (78%) of a total of 60 neurons responded with a rise in cytosolic [Ca²⁺] in the absence of extracellular Ca²⁺. To assess whether loss of cellular viability gives rise to these marked differences in Ca²⁺ transient properties, a subset of neurons were re-exposed to high [K⁺]_e in normal [Ca²⁺]_e following the [K⁺]_e test in Ca²⁺ free conditions. A representative ΔF/F₀ (t) tracing is shown in Fig 2A. After raising [Ca²⁺]_e to 2 mM, the peak amplitude of the high [K⁺]_e-evoked Ca²⁺ transient clearly exceeded that of the preceding transient recorded in the absence of external Ca²⁺, and its time course was indistinguishable from that of a response typically seen during initial exposures to high [K⁺]_e in 2 mM [Ca²⁺]_e. Identical observations were made in 7 cells. These results prove that the neurons remain viable and support the notion that the differences in Ca²⁺ transient properties between 2 and 0 mM [Ca²⁺]_e are unlikely to result from unspecific effects of the exposure to the Ca²⁺ free bath solution. At 80 mM [K⁺]_e, the average peak Ca²⁺ transient amplitude was markedly smaller in the absence than in the presence of external Ca²⁺ and their average rise and decay times were markedly prolonged compared to Ca²⁺ transients evoked in normal [Ca²⁺]_e (Fig 2B). Overall, these results suggest that a subpopulation of sympathetic neurons possess the ability to release Ca²⁺ from intracellular stores in response to prolonged membrane depolarization in the absence of extracellular Ca²⁺.

To relate the magnitude of the Ca²⁺ responses to membrane depolarization, we next recorded Ca²⁺ transients during exposure to various K⁺ concentrations. In a parallel series of experiments, we measured membrane voltage in isolated neurons, using external solutions identical to those in the Ca²⁺ imaging experiments.

Exposure to 40, 60, 80 and 100 mM [K⁺]_e in 2 mM [Ca²⁺]_e caused progressively increasing membrane depolarizations (Table 1), yielding a slope of 67.5 mV per 10-fold change in [K⁺]_e (solid line in Fig 2C). Plotting the magnitude of peak ΔF/F₀ transient amplitude against membrane potential (Fig 2D) revealed a linear increase over a range between -31.8 and -11.5 mV. Removal of Ca²⁺ from the extracellular solution did not significantly alter the resting membrane potential in 5 mM [K⁺] Tyrode's solution (Table 1). Progressive elevations in [K⁺]_e caused depolarizations that were of similar magnitude to those seen in 2 mM [Ca²⁺]_e (Table 1),

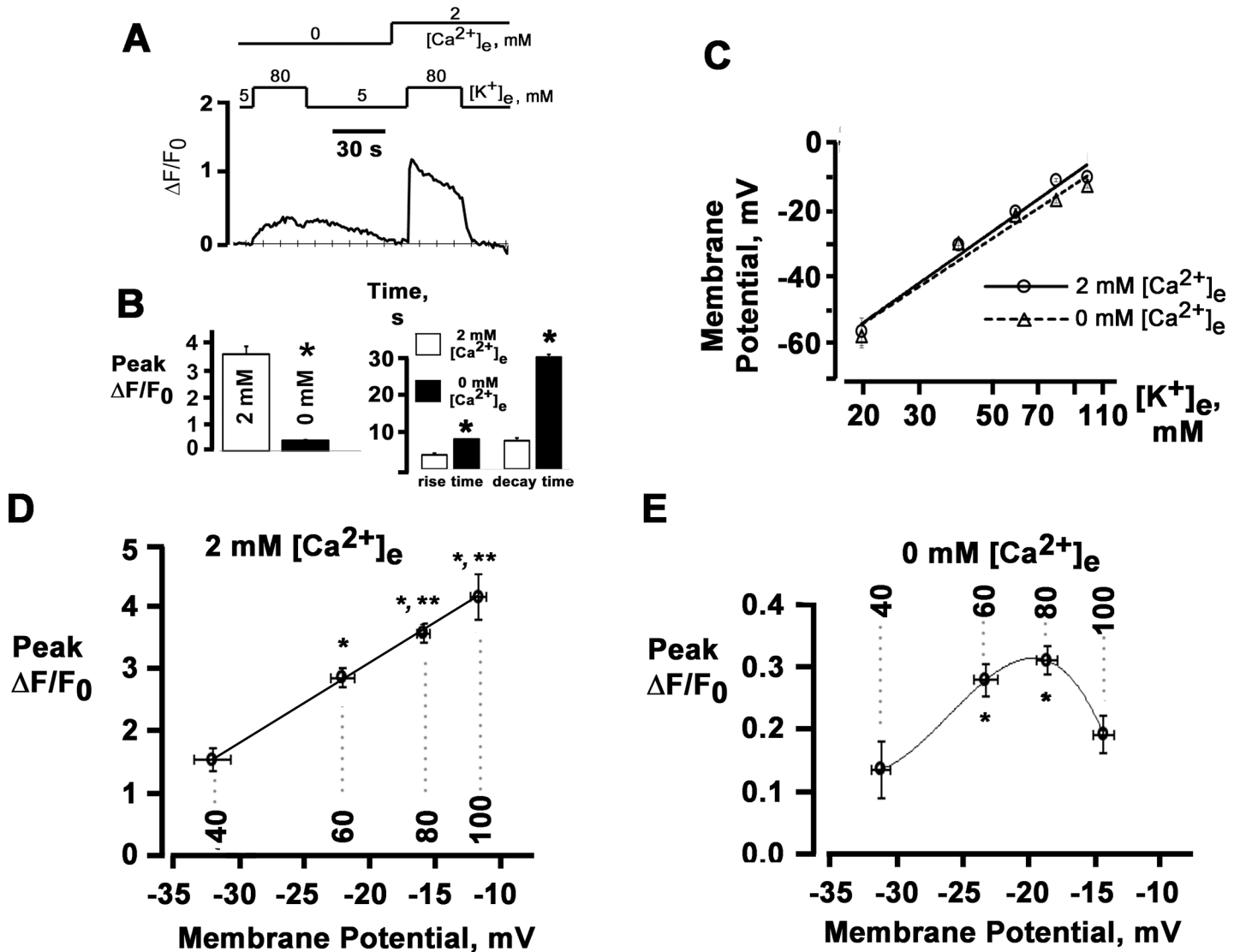


Fig 2. Sympathetic neurons possess the ability to release Ca^{2+} from intracellular stores in response to prolonged membrane depolarization in the absence of extracellular Ca^{2+} . **A:** Time course of cytosolic fluo-4 $\Delta\text{F}/\text{F}_0$ in a sympathetic neuron in response to a 30-s exposure to 80 mM $[\text{K}^+]_e$ in 2 mM $[\text{Ca}^{2+}]_e$ and a 30-s exposure to 80 mM $[\text{K}^+]_e$ in Ca^{2+} -free solution, followed by a second 30-s application of 80 mM $[\text{K}^+]_e$ in 2 mM $[\text{Ca}^{2+}]_e$ applied 70 seconds after the Ca^{2+} transient was elicited in Ca^{2+} -free solution. **B:** Bar graphs of peak magnitude of the cytosolic $\Delta\text{F}/\text{F}_0$ transients (left panel) and their rise and decay times during exposure to 80 mM $[\text{K}^+]_e$ in the presence and absence of extracellular Ca^{2+} (with 200 μM EGTA added). Rise times and decay times were measured as the intervals from 10% to 90% and from 90% to 10%, respectively, of peak $\Delta\text{F}/\text{F}_0$. Values are mean \pm SEM from 48 to 87 cells. $*P < 0.0001$ versus 2 mM $[\text{Ca}^{2+}]_e$, paired *t*-test. **C:** Plots of sympathetic neuron membrane potential as a function of $[\text{K}^+]_e$. Values are mean \pm SEM ($n = 5\text{--}8$ experiments for each $[\text{K}^+]_e$ studied). Lines are linear fits with slopes of 67.5 mV (2 mM $[\text{Ca}^{2+}]_e$) and 62.2 mV (0 mM $[\text{Ca}^{2+}]_e$) per 10-fold change in $[\text{K}^+]_e$. **D and E:** Peak magnitude of cytosolic $\Delta\text{F}/\text{F}_0$ transients as a function of membrane potential. Shown are the relationships between membrane potential and peak $\Delta\text{F}/\text{F}_0$ amplitude in response to 30-s exposures to 40, 60, 80 or 100 mM $[\text{K}^+]_e$ in 2 mM $[\text{Ca}^{2+}]_e$ (**D**) or in the absence of extracellular Ca^{2+} (**E**). Values are mean \pm SEM ($n = 18\text{--}87$ cells for each $[\text{K}^+]_e$). Solid lines represent best fits of the data to a linear function (**D**) and a polynomial function (**E**). Dashed lines denote membrane potentials generated by each $[\text{K}^+]_e$. **B:** $*P < 0.001$ versus 40 mM $[\text{K}^+]_e$; $**P < 0.03$ versus 60 mM $[\text{K}^+]_e$. **C:** $*P < 0.05$ versus 40 mM $[\text{K}^+]_e$; repeated measures ANOVA and Dunn's method for multiple comparisons.

doi:10.1371/journal.pone.0148962.g002

giving rise to a slope of 62.2 mV per 10-fold change in $[\text{K}^+]_e$ (dashed line in Fig 2C). Over the voltage range examined (-31.2 to -14.2 mV), the magnitude of peak $\Delta\text{F}/\text{F}_0$ transient amplitude displayed an inverse U-shaped dependence on membrane potential as shown in Fig 2E, which is in sharp contrast to the linear rise in peak $\Delta\text{F}/\text{F}_0$ amplitude that was observed in response to progressively increasing membrane depolarizations in 2 mM $[\text{Ca}^{2+}]_e$ (Fig 2D).

The increase in the magnitude of Ca²⁺ transient amplitude with increasing depolarization in the presence of 2 mM extracellular Ca²⁺ suggested a role of voltage-gated Ca²⁺ channel activity in governing this relationship, as had been described previously in mammalian postganglionic sympathetic neurons [10,18]. Accordingly, to relate Ca²⁺ transient properties to Ca²⁺ channel activity, we measured whole-cell Ca²⁺ currents (I_{Ca}) over a wide range of voltages including those generated by the lowest and highest [K⁺]_e used in the Ca²⁺ imaging experiments. Short depolarizations evoked Ca²⁺ currents exhibiting no, or very little, inactivation (Fig 3A). A plot of peak I_{Ca} as a function of voltage is shown in Fig 3B, exhibiting the typical bell-shaped dependence on membrane potential. The descending portion of the I_{Ca} -V curve largely coincided with the voltage range over which peak $\Delta F/F_0$ increased (see Fig 2D), suggesting that the membrane potential dependence of peak I_{Ca} controls Ca²⁺ transient magnitude over the range of membrane depolarizations studied here. This observation is in agreement with previous studies [10,18]. To examine whether depolarization-induced changes in Ca²⁺ channel gating underlie the membrane potential-dependence of peak $\Delta F/F_0$ in the absence of external Ca²⁺, we next determined the voltage-dependence of Ca²⁺ channel activation. The result is shown in Fig 3C. The probability of the channel of being activated (P_{act}) increased in a sigmoidal fashion as the membrane potential became more depolarized. This behavior contrasts with the inverse U-shaped dependence of peak $\Delta F/F_0$ on voltage in Ca²⁺-free bath solution (Fig 2E), suggesting that membrane potential-dependent changes in peak P_{act} of voltage-activated Ca²⁺ channels do not constitute the trigger for Ca²⁺ release in 0 mM [Ca²⁺]_e.

The slow kinetics of increase in [Ca²⁺]_i during sustained membrane depolarization in the absence of external Ca²⁺ (see Fig 2B) suggested the possibility that Ca²⁺ release is regulated by the steady-state activity of voltage-gated Ca²⁺ channels. The steady-state probability of a channel of being activated is the product of peak P_{act} (obtained from the activation curve in Fig 3C) and the probability of not being inactivated ($1 - P_{inact}$), i. e., steady-state $P_{act} = (\text{peak } P_{act}) * (1 - P_{inact})$. Accordingly, we next determined the voltage-dependence of I_{Ca} inactivation. Channel inactivation displayed a U-shaped dependence on voltage (Fig 3D). Fits of the descending portion of the inactivation curve to a Boltzmann distribution revealed $V_{1/2}$ and k values of -55.3 mV and 16.3 mV, respectively. Fig 3E shows the relationship between membrane potential and steady-state P_{act} . Negative to -20 mV, steady-state P_{act} increased steeply, whereas it decreased slightly at less negative potentials. Thus, steady-state activation of voltage-gated Ca²⁺ channels and peak $\Delta F/F_0$ in the absence of external Ca²⁺ shared a similar, i.e., inverse U-shaped, dependence on membrane potential over identical voltage ranges, suggesting that magnitudes of changes in the depolarization-induced [Ca²⁺]_i in 0 mM [Ca²⁺]_e are controlled by the steady-state gating of voltage-activated Ca²⁺ channels.

Depolarization in Ca²⁺ free solution induces Ca²⁺ release from IP₃-, but not ryanodine-, sensitive internal stores

To investigate the role of Ca²⁺ release from internal stores in mediating depolarization-induced increases in cytosolic [Ca²⁺], we next assessed the effects of the Ca²⁺-ATPase inhibitor thapsigargin (1 μ M) on high [K⁺]_e-evoked Ca²⁺ responses in isolated sympathetic neurons. Neurons were pre-incubated with thapsigargin for 20 min while being loaded with fluo-4/AM and then subjected to Ca²⁺ imaging in the continued presence of the inhibitor. Representative plots of $\Delta F/F_0$ as a function of time are shown in Fig 4. A 30-s exposure to 80 mM [K⁺]_e in the presence of extracellular Ca²⁺ caused an increase in cytosolic [Ca²⁺]. A second 30-s exposure to 80 mM [K⁺]_e in the absence of external Ca²⁺ did not evoke a significant increase in intracellular [Ca²⁺]. Overall, only 2 (10.5%) of 19 thapsigargin-treated neurons developed Ca²⁺ transients during exposure to elevated [K⁺]_e in the absence of extracellular Ca²⁺ compared to 47 (78%) of 60

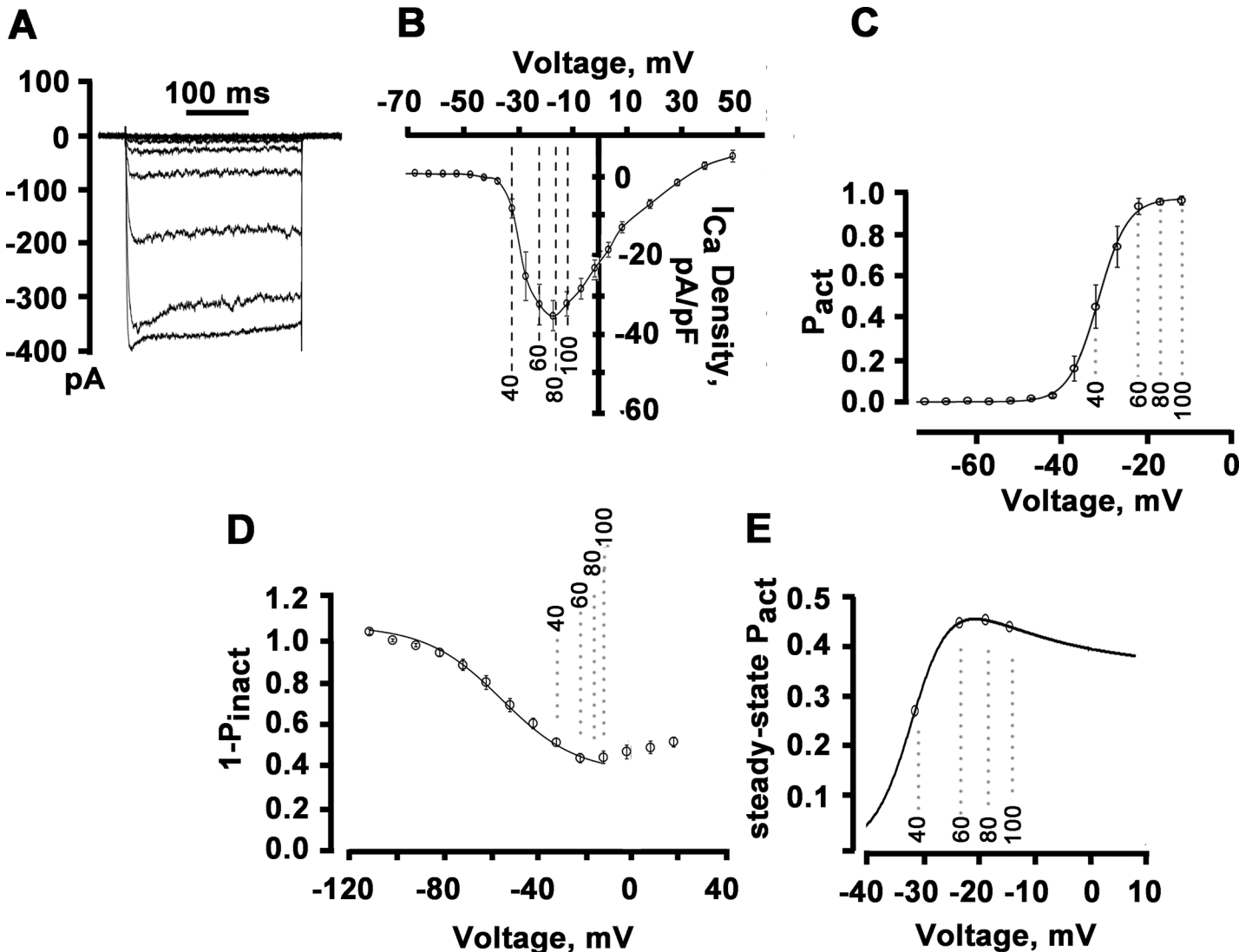


Fig 3. Peak magnitude of cytosolic $\Delta F/F_0$ transients as a function of calcium channel activity. **A:** Representative traces of whole-cell I_{Ca} recordings with 2 mM $[Ca^{2+}]_e$. Currents were elicited using 300-ms depolarizations ranging between -50 and +10 mV in 5-mV steps. Pulse interval was 10 s. **B:** Peak I_{Ca} -voltage relationship. Current amplitudes were normalized to cell capacitance and plotted as mean values. Error bars represent SEM ($n = 11$ cells). Dashed lines indicate voltages generated by each $[K^+]_e$ in 2-mM $[Ca^{2+}]_e$ bath solutions. **C:** Voltage-dependence of steady-state I_{Ca} activation, P_{act} . Values are mean \pm SEM for 11 cells. The solid line represents the mean of the best fit to each cell by a Boltzmann distribution, with $V_{1/2}$ and k values of -31.2 mV and 3.4 mV, respectively. **D:** Voltage-dependence of steady-state I_{Ca} inactivation, $(1 - P_{inact})$. For measuring voltage-dependence of inactivation, a paired-pulse voltage protocol was used consisting of a 300-ms conditioning prepulse to voltages from -90 to 40 mV followed, after a 20-ms gap at -90 mV, by a 300-ms test pulse to 0 mV. Holding potential was -90 mV and the interval between conditioning prepulses as 10 s. For generating inactivation curve, the peak amplitudes of currents evoked by the test pulse were normalized to the current evoked during each prepulse and plotted as a function of prepulse potential. Solid line is the mean of the best fit of the descending portion of the inactivation-voltage relationship (i.e., between -111.9 and 18.1 mV) to a Boltzmann function, with $V_{1/2}$ and k values of 55.3 mV and 16.3 mV, respectively. Values are mean \pm SEM ($n = 8$ cells). **E:** Calculated voltage-dependence of steady-state P_{act} of high voltage-gated Ca^{2+} channels in sympathetic ganglion neurons. The curve shows the theoretical steady-state P_{act} at any potential, using the Boltzmann values for the amount of available current and the amount of current inactivation. The maximum available current was set to 1. Circles denote values for steady-state P_{act} at voltages generated by each $[K^+]_e$ in Ca^{2+} -free bath solutions.

doi:10.1371/journal.pone.0148962.g003

non-treated cells ($P < 0.001$; Fig 4B). To make certain that membrane depolarization evoked by 80 mM $[K^+]_e$ was maintained at similar potentials among thapsigargin-treated and non-treated neurons in the study, we compared membrane potentials recorded from isolated sympathetic neurons before and during high $[K^+]_e$ -induced depolarizations in the presence of the

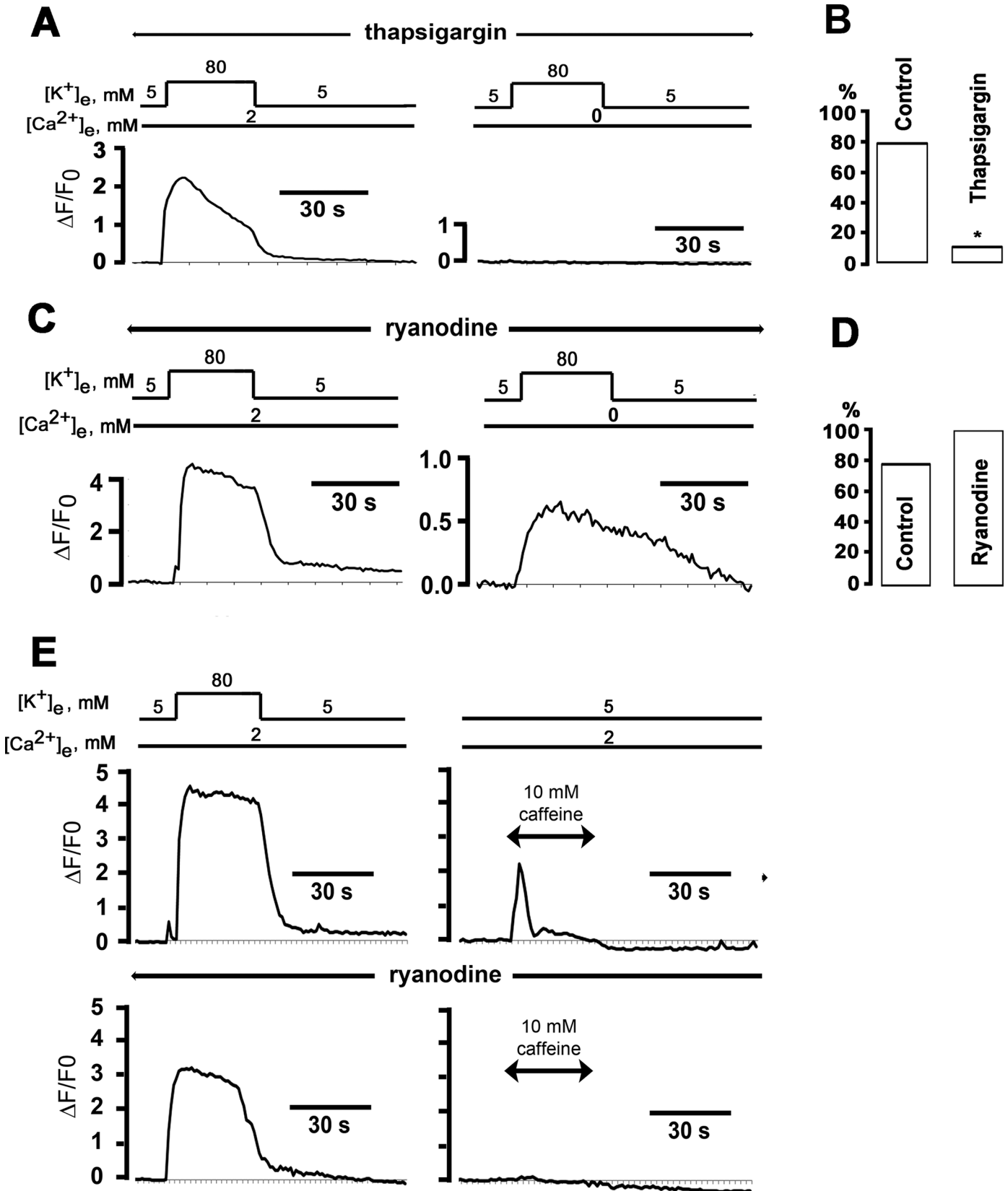


Fig 4. Thapsigargin, but not ryanodine, suppresses high [K⁺]_e-induced cytosolic Ca²⁺ transients in the absence, but not in the presence, of extracellular Ca²⁺. **A:** Time course of cytosolic ΔF/F₀ during 30-s exposures to 80 mM [K⁺]_e in 2 mM [Ca²⁺]_e (left panel) and in the absence of external Ca²⁺. To deplete internal Ca²⁺ stores, cells were continuously incubated with thapsigargin (1 μM) starting 20 min before the first exposure to elevated [K⁺]_e. **B:** Percentage of cells exhibiting [Ca²⁺]_i transients both in 2 mM and 0 mM [Ca²⁺]_e; * *P* < 0.001 versus control by Fisher Exact test (60 cells for control and 19 cells for thapsigargin). **C:** Time course of changes in cytosolic ΔF/F₀ elicited by consecutive 30-s exposures to 80 mM [K⁺]_e in normal [Ca²⁺]_e (upper panel) and in Ca²⁺-free bath solution (with 200 μM EGTA added). The cell was continuously incubated with ryanodine (20 μM) starting 20 min before the first [K⁺]_e challenge. **D:** Percentage of cells exhibiting [Ca²⁺]_i transients both in 2 mM and 0 mM [Ca²⁺]_e; *P* = non-significant versus control by Fisher's Exact test (60 cells for control and 14 cells for ryanodine). **E:** Ryanodine depletes caffeine-sensitive internal Ca²⁺ stores in postganglionic sympathetic neurons. Time course of changes in cytosolic ΔF/F₀ in response to a 30-s exposure to 80 mM [K⁺]_e followed by a 30-s exposure to caffeine (upper panel). Preincubation with 20 μM ryanodine abrogated the caffeine-, but not the high [K⁺]_e-, induced cytosolic Ca²⁺ transient (lower panel). Caffeine responses in the presence and absence of ryanodine were monitored in two different cells.

doi:10.1371/journal.pone.0148962.g004

drug with those recorded in its absence. We found no significant differences in resting membrane potential or potentials obtained during the 80-mM [K⁺]_e challenges either in normal Ca²⁺ or Ca²⁺-free bath solutions (*P* > 0.05) among the two experimental groups (Table 2). Collectively, these results indicate that thapsigargin-induced abolition of high [K⁺]_e-Ca²⁺ transients in 0 mM [Ca²⁺]_e does not result from a collapse of the membrane potential but rather supports the notion that depolarization elicits Ca²⁺ release from intracellular stores independently of Ca²⁺ influx.

Depolarization-evoked cytosolic Ca²⁺ transients in the absence of extracellular Ca²⁺ could result from conformational coupling between L-type Ca²⁺ channels and ryanodine receptors, as in skeletal muscle excitation-contraction coupling [4,19]. Accordingly, we examined the effect of pharmacological blocking Ca²⁺ release from ryanodine-sensitive stores on depolarization-induced Ca²⁺ release. We found that pretreating neurons for 20 min with ryanodine (20 μM) spared the high [K⁺]_e-induced Ca²⁺ responses both in the presence and absence of extracellular Ca²⁺ (Fig 4C). Overall, there was no significant difference in the proportion of neurons exhibiting [K⁺]-induced Ca²⁺ elevations in 0 mM [Ca²⁺]_e between the ryanodine [14 (100%) of 14 cells] and the control group [47 (78%) of 60 cells; *P* > 0.05; Fig 4D]. As a probe for ryanodine receptor function, we applied caffeine (10 mM), an agonist of ryanodine receptor-mediated Ca²⁺ release, and monitored intracellular [Ca²⁺]. Exposures to 80 mM [K⁺]_e and caffeine both reversibly elevated cytosolic [Ca²⁺]. Pretreatment with 20 μM ryanodine abrogated the caffeine response, but did not affect the high [K⁺]_e-induced response, which is consistent with previous studies (Fig 4E) [10], but differs from other studies demonstrating changes of [Ca²⁺]_i transient amplitude and/or kinetics by ryanodine [14,18]. Identical observations were made in 3 more cells. Thus, depolarization-evoked Ca²⁺ release in sympathetic ganglion neurons does not require ryanodine receptors, ruling out a skeletal muscle excitation-contraction coupling-like mechanism.

We then examined the contribution of Ca²⁺ release from IP₃-sensitive Ca²⁺ stores to depolarization-induced Ca²⁺ transients in the absence of external Ca²⁺. Previous studies had demonstrated that depolarization of insect dorsal unpaired neurons in the absence of external Ca²⁺ triggers Ca²⁺ release from IP₃-sensitive stores [6]. To determine whether IP₃ receptors

Table 2. Membrane potentials of postganglionic sympathetic neurons at rest and during exposure to 80 mM [K⁺]_e in normal [Ca²⁺]_e and in the absence of extracellular Ca²⁺ (with 200 μM EGTA added to the bath solution). Values are expressed as means ± SEM. n indicates the number of cells. There were no statistically significant differences in the membrane potential between the treatment groups (*P* > 0.05 by One Way Analysis of Variance).

Treatment	Control (mV, n = 6)	1 μM Thapsigargin (mV, n = 9)	20 μM 2-APB (mV, n = 4)
5 mM [K ⁺] _e + 2 mM [Ca ²⁺] _e	-61.8 ± 4.4	-62.1 ± 2.6	-67.7 ± 3.1
80 mM [K ⁺] _e + 2 mM [Ca ²⁺] _e	-15.7 ± 0.5	-15.3 ± 1.4	-11.1 ± 2.2
5 mM [K ⁺] _e + 0 mM [Ca ²⁺] _e	-59.9 ± 3.1	-55.6 ± 2.2	-63.4 ± 4.0
80 mM [K ⁺] _e + 0 mM [Ca ²⁺] _e	-18.5 ± 0.8	-18.8 ± 1.3	-14.6 ± 2.0

doi:10.1371/journal.pone.0148962.t002

contribute to depolarization-evoked Ca^{2+} signaling in sympathetic ganglion neurons, we pharmacologically blocked release from IP_3 -sensitive stores and then measured 80 mM $[\text{K}^+]_e$ -induced changes in cytosolic $[\text{Ca}^{2+}]_i$. We found that pretreating the neurons for 20 min with the IP_3 receptor inhibitors 2-aminoethoxydiphenyl borate (2-APB; 20 μM) or xestospongins C (10 μM) abolished the $[\text{K}^+]_e$ -evoked Ca^{2+} transient in the absence, but not in the presence, of extracellular Ca^{2+} (Fig 5A). Overall, exposure to elevated $[\text{K}^+]_e$ in 0 mM $[\text{Ca}^{2+}]_e$ induced Ca^{2+} transients in only 1 (17%) of 6 2-APB-treated and 2 (10.5%) of 16 xestospongins C-treated neurons, compared to 47 (78%) of 60 control neurons ($P = 0.001$; Fig 5B). The prevalence of non-responding cells was similar following treatment with 2-APB or xestospongins C ($P > 0.05$). Further, we found no significant differences in resting membrane potential or potentials obtained during the 80-mM $[\text{K}^+]_e$ challenges either in normal $[\text{Ca}^{2+}]_e$ or Ca^{2+} -free bath solutions ($P > 0.05$) between control neurons and neurons following IP_3 receptor blockade (Table 2). Collectively, these results support the notion that membrane depolarization in the absence of extracellular Ca^{2+} triggers Ca^{2+} release from IP_3 -sensitive internal stores, leading to slow rises in cytosolic $[\text{Ca}^{2+}]_i$.

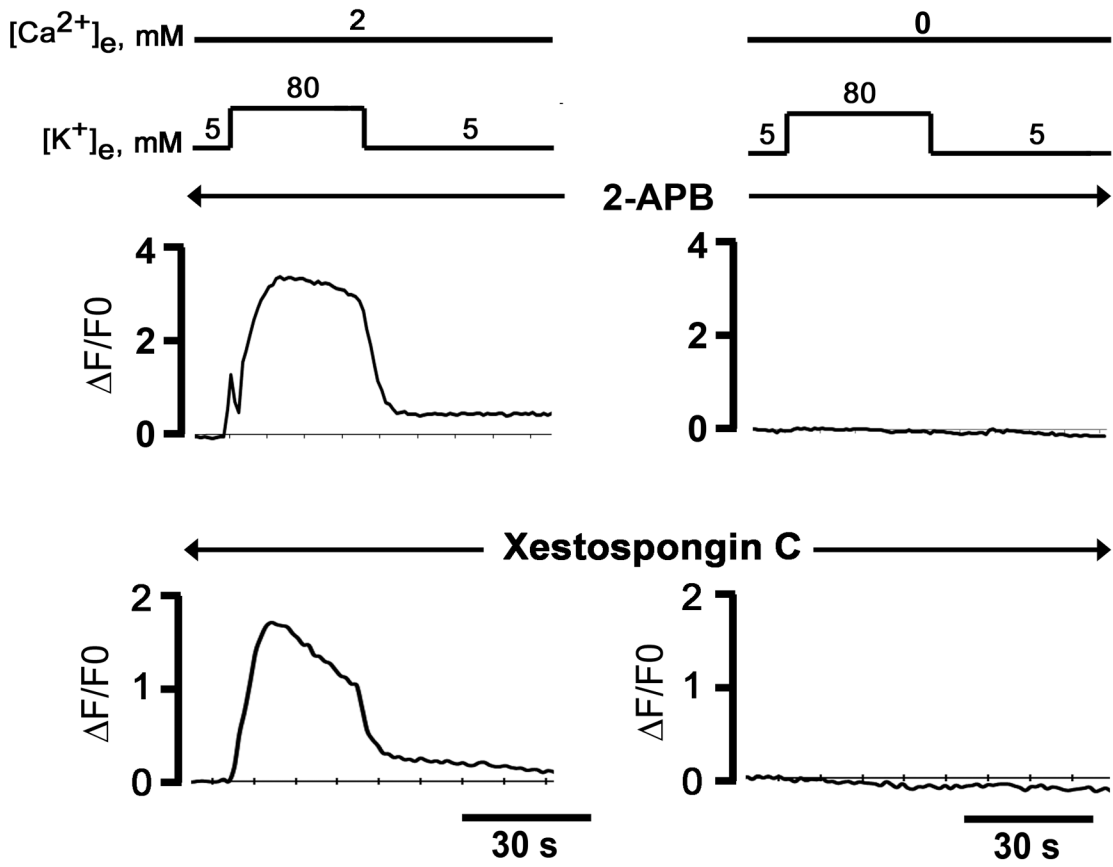
Depolarization-evoked Ca^{2+} release in the absence of extracellular Ca^{2+} does not require L-type Ca^{2+} channels

Voltage-dependent changes in L-type Ca^{2+} channel (dihydropyridine receptor) gating have previously been identified as the mechanism linking membrane depolarization to Ca^{2+} release from IP_3 -sensitive stores in skeletal myotubes in the absence of extracellular Ca^{2+} [20]. If an identical mechanism is at work in sympathetic ganglion neurons, we would expect the 1,4-dihydropyridine L-type Ca^{2+} channel antagonist nifedipine, which acts on the channel by immobilizing its gating charge, to affect depolarization-evoked Ca^{2+} transients. Measurements of whole-cell currents through high voltage-activated Ca^{2+} channels (with Ba^{2+} as charge carrier) revealed that a high concentration of nifedipine (50 μM) was required to achieve a small (~20%), yet significant, reduction in current amplitude (Fig 6A–6C). The finding that nifedipine at 10 μM did not block I_{Ba} strongly suggests a lack of functional L-type Ca^{2+} channels in adult sympathetic ganglion neurons, whereas the significant reduction of I_{Ba} at 50 μM nifedipine may reflect inhibition of $\text{Ca}_v2.x$ channels [21]. Alternatively, the insensitivity of whole-cell I_{Ba} to inhibition by nifedipine may suggest that adult sympathetic ganglion neurons express the skeletal muscle isoform of the L-type Ca^{2+} channel which has been shown previously to require nearly 50 μM nifedipine for complete block [22]. We found that pretreating neurons for 20 min with a high concentration of nifedipine (50 μM) spared the high $[\text{K}^+]_e$ -induced Ca^{2+} responses both in the presence and absence of extracellular Ca^{2+} (Fig 6D). The lack of a significant effect of nifedipine on the magnitude of depolarization-evoked Ca^{2+} transients in the presence of normal $[\text{Ca}^{2+}]_e$ is consistent with the notion that Ca^{2+} entry via L-type Ca^{2+} channels does not contribute noticeably to the rise in global $[\text{Ca}^{2+}]_i$ in our study. Overall, there was no significant difference in the proportion of neurons exhibiting $[\text{K}^+]_e$ -induced Ca^{2+} elevations in 0 mM $[\text{Ca}^{2+}]_e$ between the nifedipine [10 (100%) of 10 cells] and the control group [47 (78%) of 60 cells; $P > 0.05$; Fig 6E]. Collectively, these results support the notion that high $[\text{K}^+]_e$ -evoked Ca^{2+} release in the absence of extracellular Ca^{2+} does not require L-type Ca^{2+} channels.

Depolarization-induced $[\text{Ca}^{2+}]_i$ transients in the absence of extracellular calcium are not blocked by extracellular cadmium

Voltage-gated calcium channels become permeable to monovalent cations when extracellular calcium concentrations fall to sub-micromolar levels [23], suggesting the possibility that

A



B

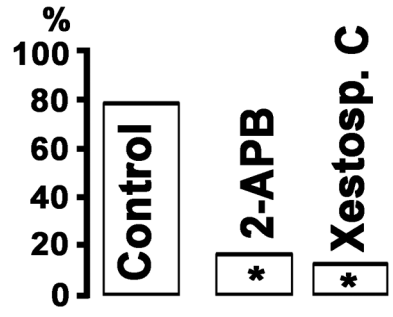


Fig 5. Pharmacological inhibitors of IP₃ receptors abrogate high [K⁺]_e-induced Ca²⁺ transients in Ca²⁺-free bath solution. **A:** Representative time courses of changes in cytosolic ΔF/F₀ in response to two consecutive 30-s exposures to 80 mM [K⁺]_e in 2 mM [Ca²⁺]_e (left panels) and in Ca²⁺-free bath solution (with 200 μM EGTA added; right panels) following 20-min incubation with 20 μM 2-APB or 10 μM xestospongine C. **B:** Percentage of neurons exhibiting [Ca²⁺]_i transients both in 2 mM and 0 mM [Ca²⁺]_e; * *P* < 0.001 versus control by Fisher's Exact test (60, 6 and 16 cells for control, 2-APB and xestospongine C, respectively).

doi:10.1371/journal.pone.0148962.g005

depolarization-induced [Ca²⁺]_i increases in the absence of external Ca²⁺ are triggered by influx of Na⁺ and/or K⁺ through open calcium channels under our experimental conditions. Accordingly, we next examined the effect of pharmacologically inhibiting ion flux through high voltage-gated Ca²⁺ channels on [K⁺]_e-Ca²⁺ transients in 0 mM [Ca²⁺]_e. Extracellular Cd²⁺ has

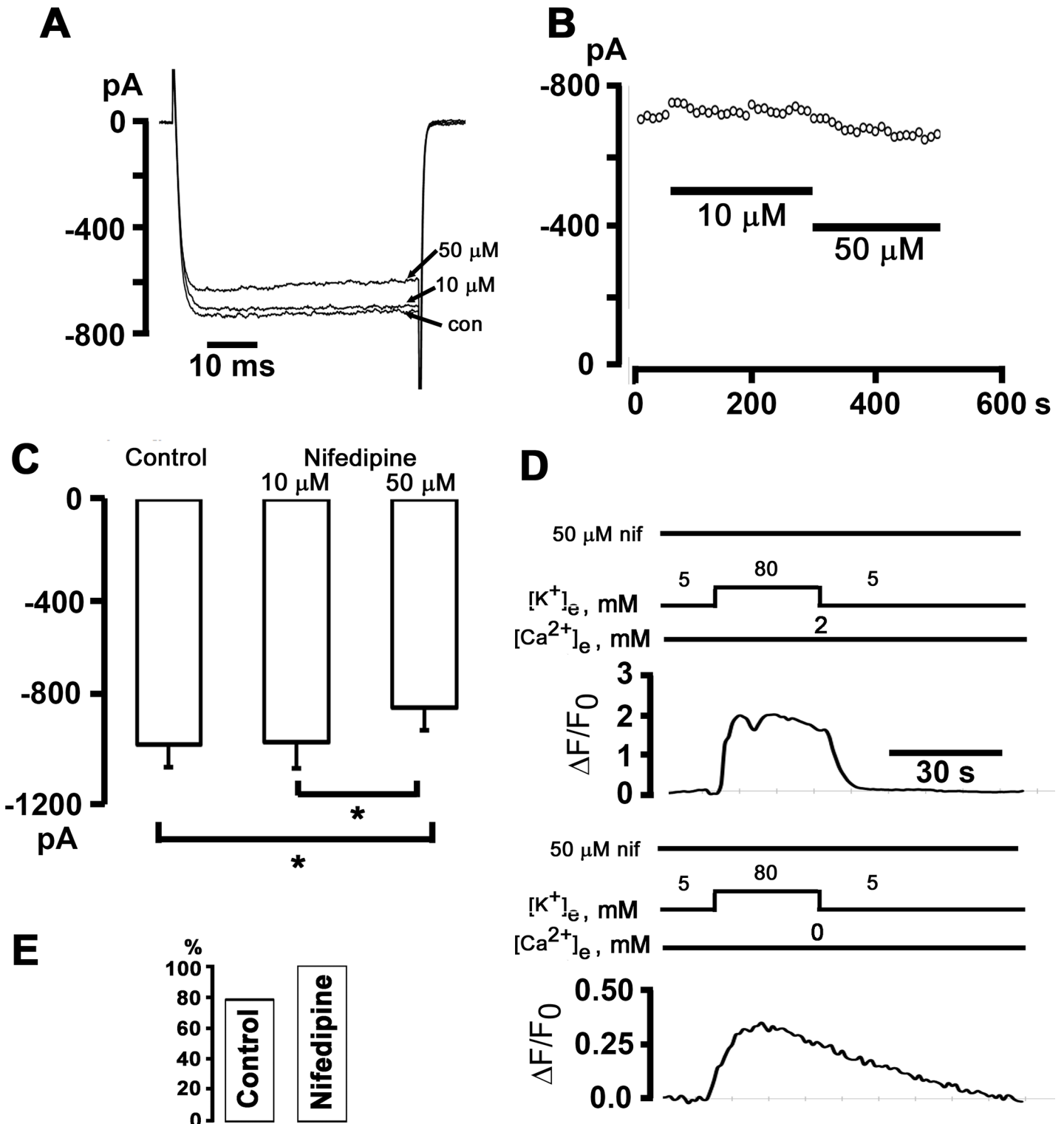


Fig 6. The 1,4-dihydropyridine antagonist of L-type Ca²⁺ channels, nifedipine, does not affect Ca²⁺ transients elicited by exposure to elevated [K⁺]_e. **A and B:** The response of peak *I*_{Ba} in a postganglionic sympathetic neuron to application of 10 and 50 μM nifedipine. *I*_{Ba} was activated by depolarizations from -80 mV to 10 mV every 10 seconds. Representative current traces are shown in A. **C:** Bar graphs represent the average peak *I*_{Ba} in control and in 10 and 50 μM nifedipine. Values are from 10 cells. **P* < 0.05, RM ANOVA on ranks followed by Student-Newman-Keuls Method for multiple comparisons. **D:** Exemplar time courses of changes in cytosolic Δ*F*/*F*₀ elicited by 80 mM [K⁺]_e in the presence (upper panel) and absence of external Ca²⁺. The cell was continuously bathed in 50 μM nifedipine starting 20 min before the first [K⁺]_e test. **E:** Percentage of cells exhibiting [Ca²⁺]_i transients both in 2 mM and 0 mM [Ca²⁺]_e; *P* = non-significant versus control by Fisher Exact test (60 cells for control and 10 cells for nifedipine).

doi:10.1371/journal.pone.0148962.g006

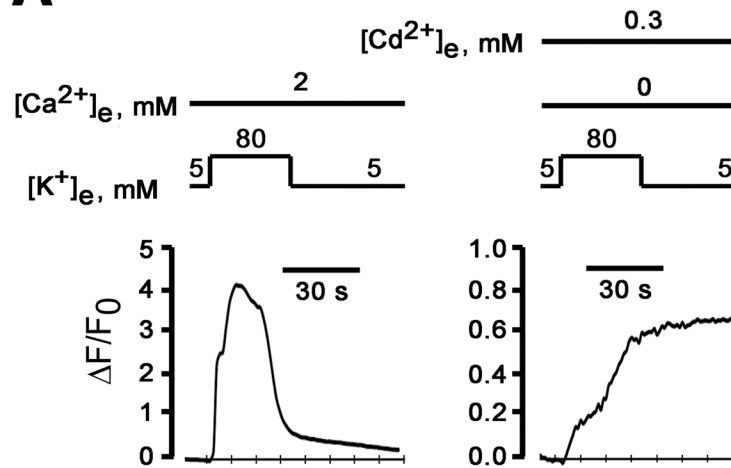
been shown previously to potently block ion flux through neuronal, high voltage-gated calcium channels in a concentration-dependent manner [10], without altering channel gating. Our measurements of whole-cell Ca²⁺ currents in voltage-clamped neurons (using Ba²⁺ as the charge carrier) confirmed the absence of resolvable inward currents following the addition of 300 μM Cd²⁺ to the bath solution (S1A–S1C Fig), supporting the notion that Cd²⁺ at this concentration potently blocked currents through voltage-activated Ca²⁺ channels, consistent with previous studies in adult sympathetic ganglion neurons [9,24]. In addition, Cd²⁺ at concentrations that block ion flux has been reported to not affect membrane potential of sympathetic ganglion neurons [10]. Thus, extracellular Cd²⁺ in micromolar concentrations should be ideally suited to distinguish a role of ion flux through versus gating of voltage-dependent Ca²⁺ channels in mediating depolarization-induced rise in [Ca²⁺]_i in 0 mM [Ca²⁺]_e. A typical ΔF/F₀ response of a sympathetic ganglion neuron to a 30-s exposure to 80 mM [K⁺]_e and 300 μM Cd²⁺ in the absence of external Ca²⁺ is shown in Fig 7A. In these conditions, high [K⁺]_e still caused an increase in ΔF/F₀, with no sign of recovery following return to 5 mM [K⁺]_e. The irreversible increase in fluo-4 fluorescence resulted from Cd²⁺ influx into the cell, because it was completely reversed by a 5-min incubation with the membrane-permeant divalent metal chelator tetrakis (2-pyridylmethyl) ethylenediamine (TPEN; 100 μM; Fig 7B), whose affinity for Cd²⁺ ($K_d = 10^{-12}$ M) [25] is several orders of magnitude higher than that for Ca²⁺ ($K_d = 10^{-4.4}$ M) [26]. The means of high [K⁺]_e-induced changes in peak ΔF/F₀ in the presence of 2 mM [Ca²⁺]_e were not significantly different before and after loading with TPEN (Fig 7C), suggesting that TPEN can be used to selectively suppress the Cd²⁺ influx-dependent component of the fluo-4 signal in our experimental conditions. Indeed, combined exposure of another TPEN-loaded neuron to 80 mM [K⁺]_e and 300 μM Cd²⁺ in the absence of external Ca²⁺ revealed the typical ΔF/F₀ response pattern seen in the absence of Cd²⁺, i.e., the increase in ΔF/F₀ readily resolved following return to physiological [K⁺]_e (Fig 7D). Identical observations were made in 4 other TPEN-loaded neurons.

To further examine whether voltage-dependent Ca²⁺ channels conduct Na⁺ currents in the absence of extracellular Ca²⁺, we sequentially measured macroscopic currents carried by these channels in 2 and 0 mM [Ca²⁺]_e. Extracellular concentrations of Mg²⁺ (2 mM) and Na⁺ (140 mM) remained unchanged. Tetrodotoxin (1 μM) was present in the bath solution throughout the measurements to block voltage-gated Na⁺ channels. Exemplar whole-cell current traces acquired in response to step depolarizations to +10 mV before and after Ca²⁺ withdrawal are shown in Fig 8A. Removal of extracellular Ca²⁺ resulted in loss of inward currents, indicating that voltage-gated Ca²⁺ channels do not carry resolvable Na⁺ currents in the ionic conditions used here. Overall, these results support the notion that depolarization-induced rises in [Ca²⁺]_i in 0 mM [Ca²⁺]_e are not triggered by ion fluxes through high voltage-gated Ca²⁺ channels.

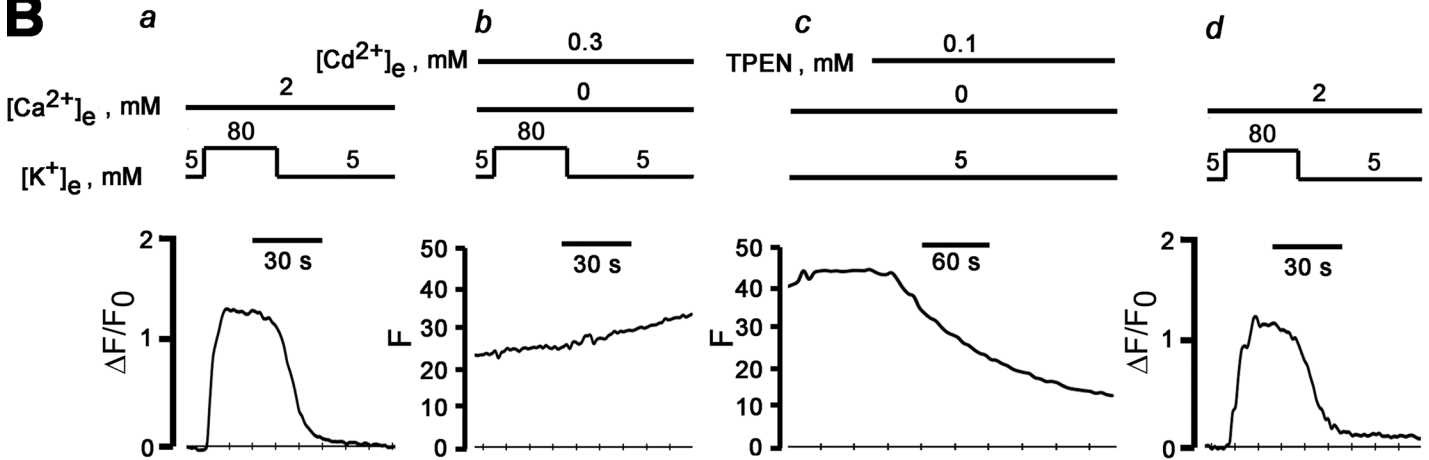
Discussion

Our results indicate that the increase in global cytosolic [Ca²⁺] seen in response to prolonged depolarization in nominally Ca²⁺-free bath solution cannot be attributed to Ca²⁺ influx and subsequent Ca²⁺-induced Ca²⁺ release. Further, a skeletal muscle excitation-contraction-like mechanism as reported previously for hypothalamic magnocellular neurons, ischemically injured spinal cord white matter, and hippocampal neurons, can be excluded as the mechanism underlying depolarization-induced Ca²⁺ mobilization [3–5]. On the other hand, our findings are similar to those reported previously by Ryglewski et al. demonstrating that insect dorsal unpaired median neurons are capable of transducing incremental depolarization into gradual

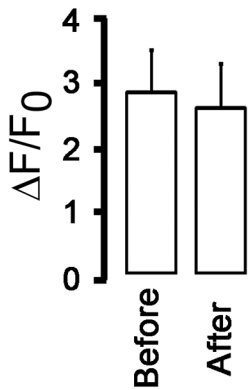
A



B



C



D

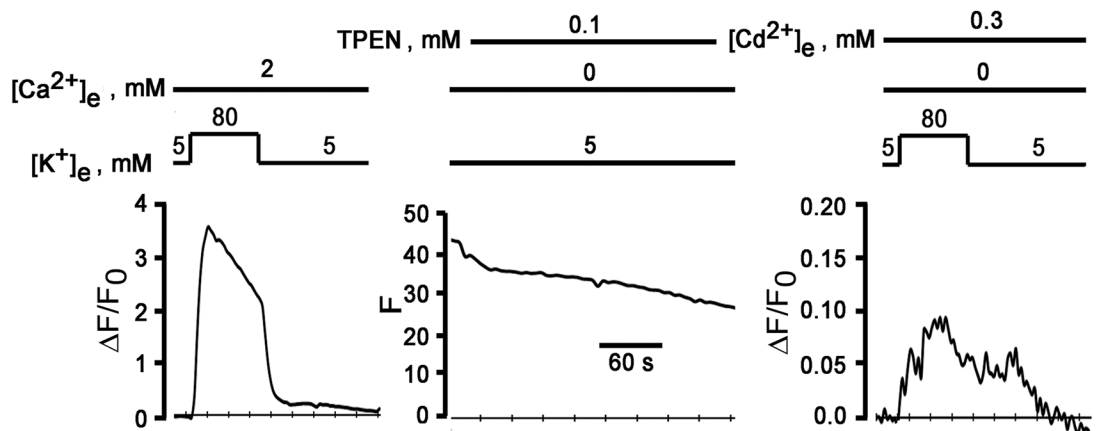


Fig 7. External Cd²⁺ does not suppress high [K⁺]_e-induced ΔF/F₀ transients in 0 mM [Ca²⁺]_e. **A:** Irreversible increase of ΔF/F₀ in depolarized neurons in the presence of extracellular Cd²⁺. Shown are time courses of changes in cytosolic ΔF/F₀ elicited by 80 mM [K⁺]_e in the presence of 2 mM Ca²⁺ (left panel) and by 80 mM [K⁺]_e and 300 μM Cd²⁺ in a Ca²⁺-free bath solution (right panel). The increase of ΔF/F₀ does not recover after removal of high-[K⁺]_e-induced depolarization. **B:** External cadmium does not block depolarization-induced increase in cytosolic ΔF/F₀ in the absence of extracellular Ca²⁺. (a) reversible increase in ΔF/F₀ in response to a 30-s exposure to 80 mM [K⁺]_e in 2-mM Ca²⁺ bath solution. (b) and (c): a second exposure to 80 mM [K⁺]_e in Ca²⁺-free solution supplemented with 300 μM CdCl₂ causes a sustained increase in fluo-4 fluorescence (b) which is not reversed until treatment of the cell with the membrane permeable metal chelator TPEN at 100 μM (c). A second K⁺ challenge of the TPEN-loaded neuron in a 2-mM Ca²⁺ bath solution (d) shows restoration of fluo-4 Ca²⁺ responsivity. **C:** Bar graphs summarizing mean ± SEM of peak cytosolic ΔF/F₀ in sympathetic neurons before and after loading with TPEN (100 μM). *P* = 0.14 by paired *t*-test (*n* = 5 cells). **D:** Extracellular cadmium does not block depolarization-induced increase in ΔF/F₀ in the absence of external Ca²⁺. Left panel: reversible increase in ΔF/F₀ in response to a 30-s exposure to 80 mM [K⁺]_e in 2 mM [Ca²⁺]_e. Following TPEN loading (middle panel), a second 30-s [K⁺]_e challenge in a Ca²⁺-free bath solution containing 300 μM Cd²⁺ gives rise to a small-amplitude ΔF/F₀ transient (right panel).

doi:10.1371/journal.pone.0148962.g007

increases in cytosolic [Ca²⁺]_i, involving Ca²⁺-influx-independent activation of a G protein-phospholipase C-IP₃ receptor pathway. However, the nature of the voltage sensor was not identified in the latter study [6].

Na-induced dissociation of G-protein subunits has been demonstrated previously in neurons [27], suggesting the possibility that high [K⁺]_e-evoked Ca²⁺ mobilization from IP₃-sensitive stores as seen in the present study involves an ion influx-dependent, but not strictly depolarization-dependent, mechanism. Specifically, Na⁺ permeation of voltage-gated Ca²⁺ channels in the absence of external Ca²⁺ is one possible pathway linking Ca²⁺ release to membrane depolarization in our experimental conditions. We think this possibility to be unlikely for several reasons. First, extracellular Cd²⁺ at concentrations that completely blocked inward currents through voltage-gated Ca²⁺ channels, did not suppress high [K⁺]_e-[Ca²⁺]_i transients

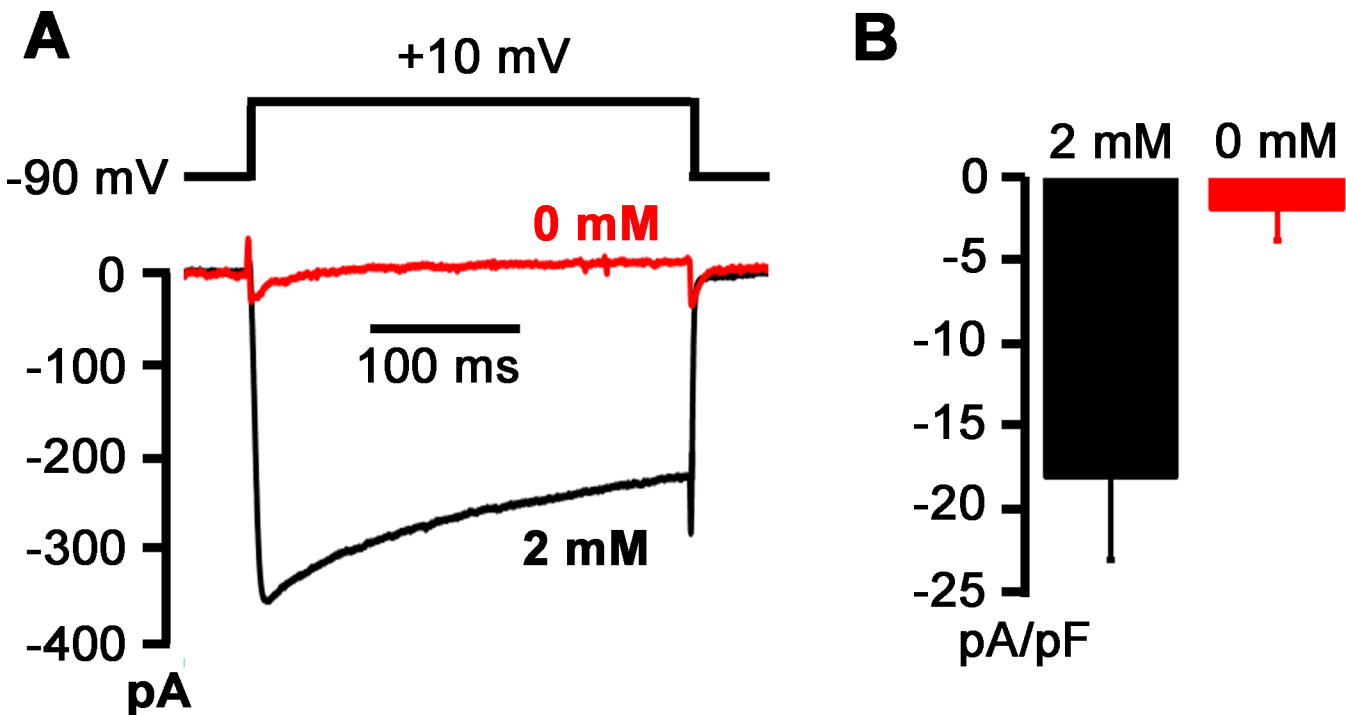


Fig 8. Voltage-gated Ca²⁺ channels do not conduct Na⁺ after removal of extracellular Ca²⁺. **A:** Exemplar whole-cell current traces sequentially recorded in a voltage-clamped neuron during 300-ms step depolarizations to +10 mV from a holding potential of -90 mV in 2 and 0 mM [Ca²⁺]_e. The bath solution also contained 1 μM tetrodotoxin to block voltage-gated Na⁺ channels. Voltages were not corrected for liquid junction potential. Numbers in mM denote extracellular Ca²⁺ concentration. Voltage-clamp protocol is shown in the upper panel. **B:** Bar graph summarizing means of peak inward currents evoked by depolarizations to +10 mV in the presence and absence of external Ca²⁺ in the same cells. Error bars represent SEM (*n* = 4 cells). *P* = 0.02 versus 2 mM [Ca²⁺]_e by paired *t*-test.

doi:10.1371/journal.pone.0148962.g008

in the absence of extracellular Ca²⁺. Second, we did not detect resolvable inward currents through voltage-dependent Ca²⁺ channels in voltage-clamped, depolarized neurons upon removal of extracellular Ca²⁺. Third, high [K⁺]_e-Ca²⁺ transients in Ca²⁺-free bath solutions could be readily evoked in the presence of 1 mM extracellular Mg²⁺, which corresponds to 4 times the IC₅₀ of Mg²⁺-induced block of Na⁺ current through N-type Ca²⁺ channels [28], the major subtype of voltage-gated Ca²⁺ channels in adult sympathetic ganglion neurons.

Also, ions other than Ca²⁺ can enter the cell via alternative voltage-modulated pathways, e.g., voltage-gated Na⁺ channels, or voltage-independent pathways, e.g., acetylcholine receptor and/or transient receptor potential cation channels. The gradual decrease in Na⁺ concentration in the bath solution for increasingly large depolarizations results in an incremental reduction in the Na⁺ driving force, progressively reducing its flux through voltage-independent channels as the membrane becomes more depolarized. This behavior conflicts with the non-monotonic dependence of depolarization-evoked peak $\Delta F/F_0$ amplitude on voltage that we observed in the absence of external Ca²⁺ (see Fig 2E). It thus appears unlikely that the magnitude of Na⁺ movement through voltage-independent pathways constitutes the trigger for Ca²⁺ mobilization in our experiments. Because the relationship between changes in membrane potential and those in extracellular K⁺ concentration followed the Nernst equation with a slope close to that expected for a K⁺-selective ion channel (see Fig 2C), the K⁺ net flux at each membrane potential achieved with various [K⁺]_e must have been zero or close to zero, excluding voltage-dependent changes in transmembrane K⁺ flux as a possible regulator of Ca²⁺ release in 0 mM [Ca²⁺]_e.

Finally, the possibility that the voltage-dependence of peak $\Delta F/F_0$ magnitude in the absence of external Ca²⁺ reflects the voltage-dependence of a steady-state current through voltage-gated Na⁺ channels has to be considered. Previous studies by others revealed the existence of a non-inactivating component of the Na⁺ current in neurons [29], whose magnitude exhibits a non-monotonic, U-shaped, dependence on voltage. However, these persistent, so-called 'window' Na⁺ currents activated at voltages significantly more negative than those of peak $\Delta F/F_0$ in 0 mM [Ca²⁺]_e, making persistent Na⁺ currents an unlikely candidate linking Ca²⁺ discharge to membrane voltage changes. Overall, our results thus support the notion that depolarization *per se* suffices to trigger Ca²⁺ discharge from IP₃-sensitive stores in 0 mM [Ca²⁺]_e.

The inverse U-shaped dependence of peak $\Delta F/F_0$ amplitude on membrane potential in 0 mM [Ca²⁺]_e is both unexpected and puzzling. Because peak P_{act} of voltage-gated Ca²⁺ channels steeply increases with depolarization over the range of membrane potentials we studied, we can exclude the possibility that gating changes as are typically achieved during peak activation of these channels, underlie voltage-induced, Ca²⁺ influx-independent Ca²⁺ release in our experiments. However, the observed non-monotonic behavior of Ca²⁺ signal strength with increasing depolarization is compatible with a mechanism, wherein the voltage-dependence of a channel's steady-state, but not peak, P_{act} serves to transduce prolonged changes in membrane potential into graded Ca²⁺ mobilization. Indeed, our numerical simulations using experimentally determined activation and inactivation properties of voltage-activated Ca²⁺ channels demonstrate that the channel's voltage-dependence of steady-state P_{act} on membrane potential overlaps with that of peak $\Delta F/F_0$ magnitude measured in 0 mM [Ca²⁺]_e. Direct proof of the role of conformational changes of a Ca²⁺ channel complex in tuning Ca²⁺ discharge from IP₃-sensitive internal stores will require experimental immobilization of gating charges in subtypes of voltage-gated Ca²⁺ channels known to be expressed in adult sympathetic ganglion neurons, including N- and P/Q-type Ca²⁺ channels. It will also require measurements of absolute free [Ca²⁺]_i levels. Because we have not calibrated the fluo-4 signal for our experimental conditions, we were unable to directly correlate changes in membrane potential to those in free [Ca²⁺]_i.

Besides voltage-gated ion channels, it is possible that non-ion channel proteins act as voltage sensors, e.g., the Na-K ATPase, the Na-Ca exchanger or the recently discovered voltage-sensitive phosphatidase, although expression of the latter in mammalian neuronal tissue has not yet been confirmed [30]. Additional studies are needed to identify the molecule capable of transducing the electrical signal into Ca²⁺ discharge from IP₃-sensitive stores in adult sympathetic neurons.

It was demonstrated previously that insect dorsal unpaired median neurons possess a membrane voltage sensor that, independent of Ca²⁺ influx, causes G-protein activation, which subsequently leads to Ca²⁺ release from intracellular stores via phospholipase C and IP₃-receptor activation [6]. It remains to be determined whether the voltage-sensitive Ca²⁺ release mechanism in our study utilizes the same signaling pathway or whether the plasmalemmal voltage-sensor directly interacts with the IP₃ receptor in the ER membrane. The slow rise in cytosolic [Ca²⁺] during prolonged depolarizations in the absence of external Ca²⁺ suggests the involvement of intermediary steps in transducing the electrical signal into a Ca²⁺ release from intercellular stores. Moreover, dihydropyridine receptors have previously been reported to act as voltage sensors for a voltage-dependent, IP₃ receptor-mediated, slow Ca²⁺ signal in skeletal muscle cells [20]. A model was proposed in which the dihydropyridine receptor decodes the electrical signal into G-protein-dependent activation of phospholipase C to produce IP₃, which then diffuses to IP₃ receptors located on the ER and nuclear membrane, ultimately activating intracellular signaling cascades. Although our experiments provide no evidence for a role of dihydropyridine receptors as voltage-sensors in depolarization-evoked Ca²⁺ release in sympathetic ganglion neurons, our data suggests that both cell types share the signaling events downstream of their respective voltage-sensor.

Although 2-APB has been shown previously to inhibit IP₃-mediated Ca²⁺ release in neurons [31], it also exerts unspecific effects on Ca²⁺ entry in non-excitabile cell types, e.g. via blockade of cation-selective channels encoded by the by transient receptor potential (TRP) genes [32]. However, our observation that xestospongine C at a concentration that has been shown previously to specifically inhibit IP₃ receptor signaling in a variety of mammalian cell types [33,34], similarly suppressed depolarization-induced increases in [Ca²⁺]_i in the absence of external Ca²⁺ support our conclusion that depolarization-evoked rises in [Ca²⁺] require functional IP₃ receptors.

Potential function of voltage-induced Ca²⁺ release in sympathetic neurons

Voltage-induced Ca²⁺ release constitutes a novel mechanism by which adult sympathetic ganglion neurons couple electrical activity to graded rises in intracellular [Ca²⁺]. The extent to which this mechanism contributes to the increase in [Ca²⁺] that normally occurs in response to single or repetitive action potentials remains to be quantitated. Eltit and co-workers previously demonstrated that tetanic stimulation of skeletal myotubes in the absence of extracellular Ca²⁺ gives rise to long-lasting, IP₃-generated, slow Ca²⁺ signals both in the nucleus and cytoplasm [34]. It will be interesting to determine whether repetitive electrical discharge of sympathetic ganglion neurons, such as occurring physiologically *in situ*, also results in slow Ca²⁺ signals similar to those evoked by high [K⁺]_e in the present study.

Although the magnitude of the depolarization-induced global Ca²⁺ transient is small compared to that of a transient elicited in normal [Ca²⁺]_e, it is possible that Ca²⁺ is released into microdomains in which it may exert strong effects on exocytosis and/or Ca²⁺-sensitive ion channels and enzymes, ultimately altering excitability, energy homeostasis, and transcriptional activity of the neuron. With regard to the latter, the elevations in nuclear fluo-4 fluorescence

that were observed to occur concomitantly with those in the cytosol both in 2 and 0 mM [Ca²⁺]_i, may play a role in transcriptional regulation [10]. The magnitude of depolarization-induced changes in nuclear fluo-4 fluorescence intensity in 2 mM [Ca²⁺]_e often reached saturation using gain settings that were optimized to monitor cytosolic fluorescence, precluding simultaneous measurements in both compartments.

Small elevations in cytosolic Ca²⁺ like those arising as a consequence depolarization-evoked IP₃-receptor stimulation, may enhance the Ca²⁺-sensitivity of nearby ryanodine receptors, thereby converting the cytoplasm in an excitable medium capable of producing regenerative Ca²⁺ responses.

Supporting Information

S1 Fig. Effect of cadmium, a non-selective blocker of voltage-gated Ca²⁺ channels, on high [K⁺]_e-induced cytosolic Ca²⁺ transients in postganglionic sympathetic neurons. A and B: Family of current traces recorded from an isolated sympathetic neuron in the absence (A) and presence of 300 μM CdCl₂ in the external solution. Currents were evoked by 200-ms voltage steps, ranging from -70 to +50 mV in 10-mV increments. **C:** Peak *I*_{Ba}-voltage relationship for the cadmium-sensitive (circles) and-resistant (squares) currents shown in A and B. CdCl₂ eliminated all inward currents. (TIF)

Author Contributions

Conceived and designed the experiments: MR. Performed the experiments: HS WT BL WT PC MR. Analyzed the data: HS WT MR. Wrote the paper: MR.

References

1. Berridge MJ. Neuronal calcium signaling. *Neuron*. 1998; 21(1): 13–26. PMID: [9697848](#)
2. Grienberger C, Konnerth A. Imaging calcium in neurons. *Neuron*. 2012; 73(5): 862–885. doi: [10.1016/j.neuron.2012.02.011](#) PMID: [22405199](#)
3. Kim S, Yun HM, Baik JH, Chung KC, Nah SY, Rhim H. Functional interaction of neuronal Cav1.3 L-type calcium channel with ryanodine receptor type 2 in the rat hippocampus. *J Biol Chem*. 2007; 282(45): 32877–32889. PMID: [17823125](#)
4. De Crescenzo V, Fogarty KE, Zhuge R, Tuft RA, Lifshitz LM, Carmichael J, et al. Dihydropyridine receptors and type 1 ryanodine receptors constitute the molecular machinery for voltage-induced Ca²⁺ release in nerve terminals. *J Neurosci*. 2006; 26(29): 7565–7574. PMID: [16855084](#)
5. Ouardouz M, Nikolaeva MA, Coderre E, Zamponi GW, McRory JE, Trapp BD, et al. Depolarization-induced Ca²⁺ release in ischemic spinal cord white matter involves L-type Ca²⁺ channel activation of ryanodine receptors. *Neuron*. 2003; 40(1): 53–63. PMID: [14527433](#)
6. Ryglewski S, Pflueger HJ, Duch C. Expanding the neuron's calcium signaling repertoire: intracellular calcium release via voltage-induced PLC and IP₃R activation. *PLoS Biol*. 2007; 5(4): e66. PMID: [17341135](#)
7. Kukwa W, Macioch T, Szulczyk PJ. Stellate neurones innervating the rat heart express N, L and P/Q calcium channels. *J Auton Nerv Syst*. 1998; 74(2–3): 143–151. PMID: [9915630](#)
8. Namkung Y, Smith SM, Lee SB, Skrypnik NV, Kim HL, Chin H, et al. Targeted disruption of the Ca²⁺ channel beta3 subunit reduces N- and L-type Ca²⁺ channel activity and alters the voltage-dependent activation of P/Q-type Ca²⁺ channels in neurons. *Proc Natl Acad Sci U S A*. 1998; 95(20): 12010–12015. PMID: [9751781](#)
9. Martínez-Pinna J, Lamas JA, Gallego R. Calcium current components in intact and dissociated adult mouse sympathetic neurons. *Brain Res*. 2002; 951(2): 227–236. PMID: [12270501](#)
10. Wheeler DG, Barrett CF, Groth RD, Safa P, Tsien RW. CaMKII locally encodes L-type channel activity to signal to nuclear CREB in excitation-transcription coupling. *J Cell Biol*. 2008; 183(5): 849–863. doi: [10.1083/jcb.200805048](#) PMID: [19047462](#)

11. Akita T, Kuba K. Functional triads consisting of ryanodine receptors, Ca²⁺ channels, and Ca²⁺-activated K⁺ channels in bullfrog sympathetic neurons. Plastic modulation of action potential. *J Gen Physiol.* 2000; 116(5): 697–720. PMID: [11055998](#)
12. Albrecht MA, Colegrove SL, Hongpaisan J, Pivovarova NB, Andrews SB, Friel DD. Multiple modes of calcium-induced calcium release in sympathetic neurons I: attenuation of endoplasmic reticulum Ca²⁺ accumulation at low [Ca²⁺]_i during weak depolarization. *J Gen Physiol.* 2001; 118(1): 83–100. PMID: [11429446](#)
13. Li BY, Schild JH. Electrophysiological and pharmacological validation of vagal afferent fiber type of neurons enzymatically isolated from rat nodose ganglia. *J Neurosci Methods.* 2007; 164(1): 75–85. PMID: [17512602](#)
14. Friel DD, Tsien RW. A caffeine- and ryanodine-sensitive Ca²⁺ store in bullfrog sympathetic neurones modulates effects of Ca²⁺ entry on [Ca²⁺]_i. *J Physiol.* 1992; 450: 217–246. PMID: [1432708](#)
15. Schoenmakers TJ, Visser GJ, Flik G, Theuvsen AP. CHELATOR: an improved method for computing metal ion concentrations in physiological solutions. *Biotechniques.* 1992; 12(6): 870–879. PMID: [1642895](#)
16. Estève E, Eltit JM, Bannister RA, Liu K, Pessah IN, Beam KG, et al. A malignant hyperthermia-inducing mutation in RYR1 (R163C): alterations in Ca²⁺ entry, release, and retrograde signaling to the DHPR. *J Gen Physiol.* 2010; 135(6): 619–628. doi: [10.1085/jgp.200910328](#) PMID: [20479110](#)
17. Satoh H, Delbridge LM, Blatter LA, Bers DM. Surface: volume relationship in cardiac myocytes studied with confocal microscopy and membrane capacitance measurements: species-dependence and developmental effects. *Biophys J.* 1996; 70(3): 1494–1504. PMID: [8785306](#)
18. Thayer SA, Hirling LD, Miller RJ. The role of caffeine-sensitive calcium stores in the regulation of the intracellular free calcium concentration in rat sympathetic neurons in vitro. *Mol Pharmacol.* 1988; 34(5): 664–673. PMID: [3193957](#)
19. Beam KG, Bannister RA. Looking for answers to EC coupling's persistent questions. *J Gen Physiol.* 2010; 136(1): 7–12. doi: [10.1085/jgp.201010461](#) PMID: [20584887](#)
20. Araya R, Liberona JL, Cárdenas JC, Riveros N, Estrada M, Powell JA, et al. Dihydropyridine receptors as voltage sensors for a depolarization-evoked, IP₃R-mediated, slow calcium signal in skeletal muscle cells. *J Gen Physiol.* 2003; 121(1): 3–16. PMID: [12508050](#)
21. Nimmrich V, Gross G. P/Q-type calcium channel modulators. *Br J Pharmacol.* 2012; 167(4): 741–759. doi: [10.1111/j.1476-5381.2012.02069.x](#) PMID: [22670568](#)
22. Bannister RA, Pessah IN, Beam KG. The skeletal L-type Ca²⁺ current is a major contributor to excitation-coupled Ca²⁺ entry. *J Gen Physiol.* 2009; 133(1): 79–91. doi: [10.1085/jgp.200810105](#) PMID: [19114636](#)
23. Hille B. Ion channels of excitable membranes. 3rd ed. Sunderland: Sinauer Associates, MA; 2001.
24. Belluzzi O, Sacchi O. Calcium currents in the normal adult rat sympathetic neurone. *J Physiol.* 1989; 412: 493–512. PMID: [2557430](#)
25. Usai C, Barberis A, Moccagatta L, Marchetti C. Pathways of cadmium influx in mammalian neurons. *J Neurochem.* 1999; 72(5): 2154–2161. PMID: [10217297](#)
26. Hinkle PM, Shanshala ED 2nd, Nelson EJ. Measurement of intracellular cadmium with fluorescent dyes. Further evidence for the role of calcium channels in cadmium uptake. *J Biol Chem.* 1992; 267(35): 25553–25559. PMID: [1281160](#)
27. Blumenstein Y, Maximyuk OP, Lozovaya N, Yatsenko NM, Kanevsky N, Krishtal O, et al. Intracellular Na⁺ inhibits voltage-dependent N-type Ca²⁺ channels by a G protein betagamma subunit-dependent mechanism. *J Physiol.* 2004; 556(Pt 1): 121–134. PMID: [14742725](#)
28. Polo-Parada L, Korn SJ. Block of N-type calcium channels in chick sensory neurons by external sodium. *J Gen Physiol.* 1997; 109(6): 693–702. PMID: [9222896](#)
29. Parri HR, Crunelli V. Sodium current in rat and cat thalamocortical neurons: role of a non-inactivating component in tonic and burst firing. *J Neurosci.* 1998; 18(3): 854–867. PMID: [9437007](#)
30. Okamura Y, Murata Y, Iwasaki H. Voltage-sensing phosphatase: actions and potentials. *J Physiol.* 2009; 587(Pt 3): 513–520. doi: [10.1113/jphysiol.2008.163097](#) PMID: [19074969](#)
31. Bootman MD, Collins TJ, Mackenzie L, Roderick HL, Berridge MJ, Peppiatt CM. 2-aminoethoxydiphenyl borate (2-APB) is a reliable blocker of store-operated Ca²⁺ entry but an inconsistent inhibitor of InsP₃-induced Ca²⁺ release. *FASEB J.* 2002; 16(10): 1145–1150. PMID: [12153982](#)
32. Xu SZ, Zeng F, Boulay G, Grimm C, Harteneck C, Beech DJ. Block of TRPC5 channels by 2-aminoethoxydiphenyl borate: a differential, extracellular and voltage-dependent effect. *Br J Pharmacol.* 2005; 145(4): 405–414. PMID: [15806115](#)

33. Bofill-Cardona E, Vartian N, Nanoff C, Freissmuth M, Boehm S. Two different signaling mechanisms involved in the excitation of rat sympathetic neurons by uridine nucleotides. *Mol Pharmacol*. 2000; 57(6): 1165–1172. PMID: [10825387](#)
34. Eltit JM, Hidalgo J, Liberona JL, Jaimovich E. Slow calcium signals after tetanic electrical stimulation in skeletal myotubes. *Biophys J*. 2004; 86(5): 3042–3051. PMID: [15111418](#)